NATIONAL ADVISORY COMMITTEE
FOR AERONAUTICS

TECHNICAL NOTE 3267

BOUNDARY-LAYER TRANSITION AT MACH 3.12 WITH AND

WITHOUT SINGLE ROUGHNESS ELEMENTS

By Paul F. Brinich

Lewis Flight Propulsion Laboratory
Cleveland, Ohio

NACA

Washington

December 1954

NATIONAL ADVISORY COMMITTEE FOR AERONAUTICS

TECHNICAL NOTE 3267

BOUNDARY-LAYER TRANSITION AT MACH 3.12 WITH AND

WITHOUT SINGLE ROUGHNESS ELEMENTS

By Paul F. Brinich

SUMMARY

Temperatures were measured on the external surface of a straight hollow cylinder alined parallel to the air stream. The stream Mach number was 3.12, the Reynolds number varied between 1×10^5 and 7×10^5 per inch, and there was negligible heat transfer between the cylinder and the stream. From the temperature measurements, it was possible to obtain laminar and turbulent recovery factors and transition locations for the cylinder with and without single roughness elements. The peak in the surface temperature was found to coincide with the mean location of the transition point as determined from schlieren observation. With no roughness element, the transition Reynolds number was found to vary approximately as the square root of the stream Reynolds number per inch. The data for the single roughness elements were correlated according to Dryden's low-speed correlation parameter; however, the present results show that three to seven times the roughness intensity is necessary at Mach 3.12 to affect transition than is required at low subsonic speeds.

INTRODUCTION

The disturbance level of several supersonic wind tunnels having various Mach numbers and Reynolds numbers has been studied in reference 1 by using an experimental technique in which the surface-temperature distribution of a thin-walled cone was measured. In reference 2 the same temperature measuring technique was used in conjunction with a statistical study of the instantaneous-transition-point location obtained from high-speed schlieren photographs. In the present report, surface-temperature measurements were utilized to study transition on a hollow cylinder alined parallel to the air flow. The investigation was conducted in the Lewis 1- by 1-foot variable Reynolds number tunnel at Mach number 3.12. The tunnel is the same as that used in the investigation reported in reference 2.

Two factors which are known from past experience to affect the location of transition in supersonic wind tunnels are density level and single surface roughness elements. In reference 3, it is shown that a change in tunnel density level corresponding to a change in Reynolds number per inch from 7×10^5 to 1×10^5 at Mach 3.05 produced a 2:1 reduction in the transition Reynolds number for cylinders similar to the one tested herein. These results were obtained by estimating the most probable location of transition from a large number of schlieren spark photographs at each tunnel density level. The first part of the present investigation was an attempt to verify by an independent method the trends of the previous schlieren results and to provide zero-roughness transition data to be used as a comparison in the subsequent analysis of roughness-induced transition. In addition, the surface-temperature measurements provided data for computing experimental laminar, transitional, and turbulent recovery factors for a flow with zero pressure gradient.

The second part of the investigation consisted of a study of the effect of single-roughness elements on transition. This study was undertaken to determine whether roughness-induced transition at supersonic speeds differed essentially from that observed at very low speeds. Previous low-speed studies of roughness-induced transition have been concerned primarily with the effects of single roughness elements, since this is a rather simple form to investigate and has some practical engineering applications. Past research on the influence of single roughness elements has been directed along the following three channels:

(1) Finding the minimum-size element which will affect the natural position of the transition point (ref. 4)

(2) Determination of the minimum-size element which will establish transition at the element (ref. 5)

(3) Estimating the effect of single roughness elements on the transition point wherever it may be (refs. 6 to 9)

For low-speed flows the desire (1) to find the smallest-size element which would affect the natural location of transition was prompted largely by practical considerations in the design and fabrication of laminar-flow airfoils. It is for precisely the same reason that such a study would be of interest at supersonic air speeds.

Knowledge of the conditions (2) required to establish transition at a roughness element is of particular interest in boundary-layer studies in which it is desired to simulate boundary layers which are completely turbulent. Another application may be in preventing laminar separation near the inlets of supersonic diffusers by producing a turbulent boundary layer in the regions of strong adverse pressure gradients.

Knowledge of the more comprehensive objective (3), the determination of the effect of single roughness elements on the transition point wherever it may be, is probably of greater value in understanding the fundamental role of roughness in promoting transition, since it automatically includes objectives (1) and (2). In the present case, the experimental data to be presented will make it possible to evaluate the validity of various low-speed correlations for use at supersonic speeds.

SYMBOLS

The following symbols are used in this report:

C, C_1, C_2 numerical constants

k height of roughness element, in.

L screen mesh size

M Mach number

P pressure coefficient, $P = \dfrac{p - p_\infty}{q}$

Pr Prandtl number

p static pressure

q dynamic pressure, $\dfrac{1}{2}\rho_\infty u_\infty{}^2$

R temperature recovery factor, $R = \dfrac{T_W - T_\infty}{T_0 - T_\infty}$

Re_t transition Reynolds number, $\dfrac{u_\infty x_t}{\nu}$

$Re_{t,0}$ transition Reynolds number for zero roughness, $\dfrac{u_\infty x_{t,0}}{\nu}$

T absolute temperature

u velocity

u' turbulent velocity perturbation in free stream (rms value)

u_k velocity at distance k from surface in absence of element

u_τ shear velocity, $u_\tau = \sqrt{\dfrac{\tau_W}{\rho_\infty}}$

x distance from leading edge, in.

x_k distance from leading edge to roughness element, in.

x_t distance from leading edge to transition point, in.

$x_{t,0}$ distance from leading edge to transition point for zero roughness, in.

δ^* displacement thickness of boundary layer, $\delta^* = \int_0^{\delta} \left(1 - \dfrac{\rho u}{\rho_\infty u_\infty}\right)dy$

δ_k^* displacement thickness at x_k in absence of roughness element

Λ' Taylor's fluctuating pressure-gradient parameter (ref. 13)

ν kinematic viscosity in free stream

ρ mass density

τ frictional shear stress

Subscripts:

0   stagnation conditions

w   wall conditions

∞ free-stream conditions

APPARATUS AND PROCEDURE

Surface-temperature measurements were made on a hollow circular cylinder with an outside diameter of 5.31 inches and an over-all length of 33 inches. The construction consisted of a thin outer shell supported on an inner hollow cylinder, strut-mounted from the tunnel wall. Between the outer shell and the cylinder was a Fiberglas heat insulating bushing. Pertinent construction details and dimensions are given in figure 1.

The outer shell was made of 0.030-inch-thick 18-8 stainless steel. The shell was formed by rolling from flat stock and butt welding along the length. The finishing operation consisted of spinning on a mandrel, polishing, and turning the 5° internal bevel at the leading edge. The leading edge was approximately 0.006-inch thick, which is about the minimum thickness consistent with the prevention of buckling for the material used. The height of the polished-surface irregularities had a value of about 12 microinches, root mean square.

Temperature measurements on the outer shell were obtained from 50 stainless-steel - constantan thermocouples located at 1/2-inch intervals along a generator of the cylinder beginning at a point $1\frac{1}{2}$ inches from the leading edge. The stainless-steel - constantan thermocouples on the model were formed by soft-soldering constantan thermocouple wire into small holes drilled in the thin stainless-steel shell. A self-balancing-type potentiometer with a 1-millivolt total-scale deflection was used for measuring the thermocouple voltage. The reference junction was maintained close to room temperature.

In order to obtain temperature distributions along various generators of the cylinder, provisions were made for rotating the outer shell. Thus it was possible to determine whether transition occurred at a given longitudinal position all around the model for a given test-section Reynolds number.

The roughness elements which were used to promote transition consisted of six rings made of the following sizes of wire: k = 0.005, 0.010, 0.020, 0.032, 0.052, and 0.079 inch. These rings were used singly and were located in various positions along the model. They were formed by pulling a loop of wire taut about the model and soft-soldering a lap joint. The wires were maintained in position by friction.

Tests were run in the 1- by 1-foot variable Reynolds number wind tunnel at Mach 3.12. This is the same test facility used in earlier boundary-layer measurements on cylinders reported in reference 3, although the original small entrance reservoir was replaced with a large reservoir having turbulence damping screens and a honeycomb flow straightener. These two entrance reservoirs are described in reference 2, where a comparison is made of transition phenomena on a conical model tested in both the original and revised tunnel arrangements.

Stagnation pressures in the tunnel reservoir were varied from about 7 to 50 pounds per square inch absolute. Stagnation temperatures were maintained about 50° F ($+12^{\circ}$, -6°) and were sufficiently steady ($\pm 0.5^{\circ}$ F) so that successive temperature measurements along the model length could be made under substantially constant stagnation conditions. The range of Reynolds number per inch in the test section was 1×10^{5} to 7×10^{5}.

Temperature distributions along the model were obtained by successively reading the temperature at each thermocouple beginning at the leading edge. Total elapsed time for reading 50 thermocouples was about 1 minute. Most of the transition locations were obtained by reading the temperature only in the vicinity of the temperature peak, which was found to occur at the mean of the transition-point locations as indicated by simultaneous schlieren photographs of the boundary layer. The light source used to obtain the schlieren photographs had a duration of about

3273

1 microsecond; hence the resulting photographs showed the instantane-
ous position of the transition point, whereas the temperature measure-
ments gave a statistical average position.

The estimated absolute error in the temperature measurements was
approximately $\pm 0.25^\circ$ F, whereas the relative error was only $\pm 0.10^\circ$ F.
The probable error involved in measuring transition locations on indi-
vidual schlieren photographs was less than ± 0.5 inch.

PRELIMINARY CONSIDERATIONS

Before an accurate evaluation of the effect of density level and
roughness elements on transition location can be made, it is first nec-
essary to consider the possible influence of other parameters which
are also known to affect transition. These are (1) pressure gradient,
(2) turbulence level, (3) heat transfer, (4) Mach number, (5) shock
waves in the flow, and (6) leading-edge bluntness.

An examination of the pressure-coefficient distributions over the
model (fig. 2) indicates that a small favorable pressure gradient
$(\frac{dP}{dx} = -0.005/\text{in. approx.})$ existed forward on the model up to $x = 5$ inches.
From $x = 5$ to $x = 11$ inches, the gradient was unfavorable and had a
value of 0.001 per inch. These were the minimum and maximum gradients
observed over that part of the cylinder where the flow might be laminar.
Gradients of such magnitude have been shown to be negligible in establish-
ing certain criteria for complete stability of the laminar boundary
layer, as in reference 10. The pressure gradients encountered in the
present tests may therefore be inferred to have little, if any, effect
on the location of transition.

Hot-wire turbulence intensity measurements were made in the entrance
of the tunnel contraction where the free-stream velocity was about 120
feet per second. A plot of turbulent intensity u'/u_∞ against Reynolds
number per inch u_∞/ν is given in figure 3. The lowest values of tur-
bulent intensity were measured at the highest and lowest density levels,
and a maximum intensity of 1 percent was noted at an intermediate density
value. With the turbulence at the beginning of the tunnel contraction
assumed isotropic, a computed value for the turbulent intensity in the
test section may be found according to reference 11. By neglecting the
effect of viscous decay of turbulence, the influence of the tunnel con-
traction is to yield an estimated value of the turbulent intensity for
the test section of only 6 percent of the initial value at the entrance.
It should be noted, however, that this computation does not take into
account any subsequent generation of turbulence within the test section,
for example, turbulence propagated along Mach lines by the fluctuations
in the turbulent tunnel-wall boundary layer.

Heat-transfer effects due to differences in wall temperature inside and outside the model are negligible since the calculated wall temperatures differed by only 3° F, and a thermal insulating bushing was interposed between the inner and outer walls. Likewise, the test-section Mach number variation with Reynolds number per inch was only ± 0.01 with a mean value of 3.12. The possibility of premature transition caused by shock waves in the flow is considered remote, since the leading-edge shock and those off the roughness elements were generally reflected back on the model at substantial distances downstream of the transition point. Other shock waves in the flow were of smaller consequence.

Slight variations in the leading-edge shape caused by dust-particle inpingement were responsible for small changes in the transition position. The effect of such variations was minimized by a day-to-day removal of leading-edge burrs with an oilstone.

It is therefore concluded that the effects of pressure gradient, heat transfer, Mach number variation, shock disturbances, and leading-edge-thickness variations played no important part in locating transition in the present experiments. In view of the questionable nature of the turbulence intensity in the test section, however, the specific effect of turbulence level on transition could not be determined in the present investigation.

RESULTS AND DISCUSSION

Before presenting the principal results of this investigation, it is necessary to establish a relation between the observed surface-temperature distribution and the location of the transition point. Reference 1 gives a method for defining the start of transition on a cone when the surface-temperature distribution is known; this may be illustrated with the aid of figure 4. One of the curves is a typical recovery-factor distribution for a 10° included-angle cone (ref. 2). The start of transition as defined in reference 1 corresponds to the intersection at point A, which is the point where the recovery temperature begins a sharp rise after having maintained a relatively constant laminar value.

A typical recovery-factor distribution for the cylinders shown in figure 5 displays a different behavior from that observed on the cone, however. Because of the peculiar variation in recovery factor on the forward portion of the cylinder, it is doubtful whether a location for the start of transition as defined in reference 1 could be obtained from this distribution. The gradual rise in recovery factor on the forward part of the cylinder has suggested the possibility of heat-conduction effects along the outer stainless-steel shell. The result of a heat-transfer calculation to evaluate these effects showed, however, that they could not account for the gradual rise in surface temperature. Furthermore, structural differences between the cone and the cylinder

were not great enough to cause large differences in heat transfer by con-
duction. The reason for the gradual rise in the recovery factor on the
forward portion of the cylinder has not yet been established. Although
the cylinder was tested in the same air stream as the cone, the local air
stream over the respective surfaces (and hence the local turbulence level)
may have been sufficiently different to cause the different temperature
distributions. Another possibility is that this phenomenon may be associ-
ated with disturbances of the boundary layer produced by the leading edge,
because the leading edge constitutes the chief difference between cylinder
and cone geometry.

Despite the unexplained nature of the temperature distribution,
however, comparison of the transition-point location obtained from
schlieren photographs indicates that the temperature peak corresponds
very closely to the most probable location of the transition point ob-
tained from the schlieren observations. This temperature-peak location
will therefore be assumed to be a significant point in the transition
process and will be referred to as the transition point.

Recovery-factor distribution without roughness. - Temperature re-
covery factors R along the cylinder are plotted in figure 5 for sev-
eral values of Reynolds number per inch. These recovery factors were
obtained along the bottom of the model and may be taken as typical of
the distributions found along six other cylinder generators. The only
significant difference noted along the various generators was a slight
forward displacement of the temperature peak on the side of the model
relative to the top and bottom.

Included in figure 5 for comparison are the theoretical laminar and
turbulent recovery factors. The laminar recovery factor was computed
from the equation

$$R = \sqrt{Pr}$$

where the Prandtl number Pr was evaluated at an arithmetic mean tem-
perature between the stream static and wall values. This gave a value
of Pr = 0.740 and R = 0.860. Turbulent recovery factors were found
from the analysis of reference 12, with the assumption of a $1/7^{th}$ power
turbulent velocity profile and with the Prandtl number again evaluated
at the arithmetic mean temperature. The turbulent recovery factor was
found to be 0.885.

Figure 5 indicates that the experimental laminar recovery factors
are higher than theoretical and that the experimental turbulent recovery
factors are generally lower than theoretical. As the Reynolds number
per inch is diminished, the agreement between experiment and theory
improves in both the laminar and turbulent regions until at u_∞/ν =
1.0×10^5 per inch there is little difference between the two. Also

3273

2-2-CS

indicated in the figure are transition locations obtained from schlieren photographs, and these are all seen to correspond rather closely with the temperature peaks.

Transition without roughness. - In order to study in greater detail the shift of the transition point as the tunnel density was varied, some of the temperature surveys were made only in the vicinity of the temperature peaks but at a large number of values of u_∞/ν The x locations of the temperature peak along the bottom and side of the cylinder as a function of u_∞/ν are presented in figures 6(a) and (b), respectively. Data from several runs are presented in each figure to illustrate the degree of consistency which was maintained during the course of the test. Differences between the various runs are probably caused by small displacements of the model after making necessary adjustments and repairs or by acquiring small nicks in the leading edge during a run. In no case are the differences in transition location greater than 1.0 inch. When no nicks developed on the leading edge and the model was not disturbed in any way, transition locations could be duplicated from day to day with an accuracy of ±0.1 inch. Hence this method for determining transition location may be regarded as relatively precise and having, in addition, elements of dependability and simplicity.

The transition locations in figure 6 show a downstream movement as the Reynolds number per inch is diminished, a qualitative result to be expected. At $u_\infty/\nu = 2\times10^5$ per inch, a slight reversal in the movement of transition is apparent, particularly for the data on the bottom of the model (fig. 6(a)). No explanation for this reversal in the transition-point movement is known.

When the transition locations in figure 6 are expressed in terms of the transition Reynolds number Re_t, figure 7 is obtained. This figure verifies the downward trend in Re_t with decreases in Reynolds number per inch noted in reference 3. · There is almost a three-fold reduction in Re_t for a seven-fold reduction in tunnel density. Both sets of data show approximately the following variation in transition Reynolds number:

$$Re_t = C\sqrt{u_\infty/\nu}$$

where the value of C is 5100 (in.)$^{1/2}$ for the top of the model and 4150 (in.)$^{1/2}$ for the bottom. These values of C are valid, of course, only for the present investigation and should be expected to differ for other stream turbulence levels, Mach numbers, leading-edge thicknesses, and model configurations.

It is of interest to note that the variation for the transition Reynolds number expressed by the above equation can be obtained from Taylor's hypothesis concerning transition induced by fluctuating pressure

gradients in the stream turbulence (ref. 13) provided two assumptions are made. According to reference 13, the fluctuating-pressure-gradient parameter Λ' for which transition on a flat plate takes place is given by

$$\sqrt{\overline{\Lambda'^2}} \propto x_t \left(\frac{u'}{u_\infty}\right)^2 \sqrt{\frac{u'}{L\nu}} = f(Re_t)$$

The two assumptions made in the present analysis are (1) the turbulence in the test section has a constant value for all density levels, and (2) the critical value of the fluctuating-pressure-gradient parameter Λ' for transition is a constant. The first assumption is made in view of meager evidence to the contrary and should be regarded as hypothetical. The second assumption, that Λ' is a constant for the range of present test conditions, has been made in low-speed flow experiments (e.g., ref. 5) where correlation of transition locations has thereby been obtained. Making the above assumptions and taking L, the tunnel screen mesh size, as a constant yield the following expression:

$$Re_t = C\sqrt{u_\infty/\nu}$$

which is identical to the variation of transition Reynolds number found experimentally.

An interesting comparison of some independent data obtained on a cylinder similar to the one investigated herein (ref. 14) is included in figure 7(a). These data were obtained at six Mach numbers ranging from 2.15 to 5.01 in a 40- by 40-centimeter blowdown tunnel having stagnation pressures equal to atmospheric. The rather common assumption is made in reference 14 that variations in the transition Reynolds number are the result of changes in Mach number. Figure 7(a) shows that the variations in Re_t can be correlated with the present results when plotted against u_∞/ν. Consequently, it appears that the influence of stream Reynolds number on transition may be more significant than the effect of Mach number.

Transition caused by roughness. - The temperature measuring technique used above to find the location of the transition point without roughness was found equally satisfactory when transition was caused by single surface roughness elements. Again schlieren spark photographs indicated that the most probable transition location coincided with the observed temperature peaks.

Transition-point locations obtained from peak temperature measurements as a function of Reynolds number per inch u_∞/ν are given in figure 8 for six element sizes (k = 0.005, 0.010, 0.020, 0.032, 0.052, and 0.079 in.) located at various positions along the model. Also included are transition-point locations for zero roughness (indicated by solid curves). These curves were obtained from data taken at approximately

the same time that the corresponding roughness data were obtained. The variations in the zero-roughness curves from one figure to the next correspond to the variations noted in figure 6.

Certain general trends may be deduced from these figures. As in the case for zero roughness, decreases in u_∞/ν caused downstream movement of the transition point. Exceptions to this behavior occurred when transition would tend to remain fixed at the roughness element for a certain range of u_∞/ν before moving downstream with reductions in u_∞/ν.

For an element initially located upstream of the transition point, any movement of the element toward the leading edge produced an upstream movement of the transition point. An element located downstream of the transition point, however, had no effect on transition, that is, the transition point had the same location as for the case of zero roughness.

Another trend to be noted is that any increase in the size of the roughness element initially located upstream of the transition point produced a displacement of the transition point toward the leading edge until it reached the element. Again, if the element size were varied when the element was in the turbulent region, no effect on the transition point was noted.

Most of the above trends may be anticipated from transition experiments at low speeds (e.g., refs. 5, 6, and 8). An exception to these trends was found in reference 7, where it was conjectured that the location of the roughness element had no effect on transition location; only the size of the element was of importance. The present data indicate clearly that both the size and the location of the element have large effects in positioning transition.

Certain peculiarities in the data of figure 8 should be noted. The inflection point at $u_\infty/\nu = 2\times10^5$ per inch for the case of zero roughness tends to persist even though transition is displaced considerably by the roughness element. This may be seen in figure 8(d) for the 0.032-inch element at $x_k = 6.0$ inches. In figures 8(a), (b), and (c) it seems that the value of $u_\infty/\nu = 2.0\times10^5$ per inch is a lower bound beyond which it becomes more difficult to affect transition with the smaller sizes of roughness elements, regardless of how far forward they are moved.

Another anomaly which contradicts one of the aforementioned general trends was an occasional slight increase in x_t when the element was placed in the turbulent region $(x_t > x_{t,0})$. An example of this occurred in figure 8(c) for the 0.020-inch element located at $x_k = 8.0$ inches at values of $u_\infty/\nu > 3\times10^5$ per inch. Since this was a relatively rare behavior, it was disregarded in the analysis which follows, and transition was assumed to be unaffected by roughness elements located in the turbulent boundary layer. Such peculiarities in behavior may have been caused by slight changes in leading-edge shape during a particular test run.

One more peculiarity in these data deserves notice. Whenever transition approached close to an element, it became difficult to separate the temperature rise caused by the element and that caused by transition. Hence, the temperature peak occasionally became fixed at the element and x_t appeared to have a larger value than with zero roughness. In this ambiguous case it was assumed for the analysis of the data which follows that transition never occurred downstream of the zero-disturbance location.

Analysis of roughness results. - Two of the criterions that have been proposed in the low-speed transition literature for finding the minimum-size element necessary to establish transition at the roughness element are expressed by the formulas

$$ku_k/\nu = C_1$$

and

$$ku_\tau/\nu = C_2$$

The velocity in the absence of the element at the height k above the surface is denoted by u_k. The quantity u_τ is the shear velocity at the transition point and is defined by

$$u_\tau = \sqrt{\tau_w/\rho_\infty}$$

(The physical quantities appearing in this and the subsequent roughness analysis are shown in fig. 9.) Typical values of C_1 and C_2 given for low-speed results are

$$C_1 \sim 400 \qquad (\text{refs. 4 and 5})$$

$$13 < C_2 < 20 \qquad (\text{refs. 7 and 8})$$

Analogously, criteria have been given for finding the minimum-size roughness element which affects the natural (zero roughness) location of transition. Reference 7 proposes a value of $C_2 = 7$ from data obtained at low speeds. The above criteria apply only to roughness elements having a circular cross section (wires). Substitution of a smoothly shaped bulge or hollow of equal height for a wire element may increase the above values tenfold (ref. 4). Likewise, substitution of square sectional elements of equal height may decrease the above constants because of a larger disturbing effect on transition.

In figures 10 and 11 are presented values of ku_k/ν and ku_τ/ν against u_∞/ν obtained from the data of figure 8. Values of ku_τ/ν were computed by using the equation

3273

$$ku_\tau/\nu = 0.567\ k\left(\frac{u_\infty}{\nu}\right)^{3/4}\left(\frac{1}{x}\right)^{1/4} \tag{1}$$

When $k < \delta_k$, u_k was obtained from the flat-plate boundary-layer solution of reference 15. The solid symbols denote minimum-size element to establish transition at the element; the open symbols denote minimum-size element which affects the natural location of the transition point.

The results of figures 10 and 11 exhibit large variations in ku_k/ν and ku_τ/ν for changes in the parameters u_∞/ν and k. The large variation with u_∞/ν is caused by the failure of the two criterions to take into account the natural location of transition without roughness elements. The variation with the parameter k alone indicates that the roughness height should enter not as an absolute linear dimension but as a ratio with the boundary-layer thickness. A comparison with the low-speed results shows absolutely no agreement. The values of ku_k/ν and ku_τ/ν found for $M = 3.12$ are from 5 to 100 times as large as those commonly accepted at low speeds.

A correlation based on a variation of one of the above parameters has been suggested. If the element size k is omitted in the parameter ku_τ/ν plotted in figure 11, an apparent straight-line relation (on a logarithmic plot) is found to exist between u_τ/ν and u_∞/ν. The resulting plot approximately represents the correlation of figure 7 but in different notation. However, the detailed behavior of the points for the minimum-size element required to fix transition at the element is masked by the insensitivity of $(1/x_t)^{1/4}$ (eq. (1)) to changes in the location of the transition point. In addition, such a correlation has no physical significance insofar as the effect of roughness-element size on transition location is concerned.

Whereas the foregoing analyses consider only the maximum and minimum effects of roughness on transition, several attempts have been made to correlate intermediate effects as well. Rather recent attempts at correlation are given in references 6, 7, 9, 16, and 17. The correlation proposed in reference 7 has already been dismissed because it attributed no significance to the element location. Reference 9, which is an adaptation of Taylor's hypothesis to roughness-induced transition, proposed a correlation obtained with low-speed data which was tested with the present data for the 0.052-inch element only. This attempt at correlation was unsuccessful.

The correlation proposed by Dryden in reference 6 and which was checked independently with results presented in reference 17 for low-speed flows and in reference 16 to a very limited degree for high-speed flows was applied to the present data. This correlation is expressed by the following equation:

$$\frac{Re_t}{Re_{t,0}} = \frac{x_t}{x_{t,0}} = f(k/\delta_k^*) \qquad\qquad (2)$$

where the subscript 0 refers to the zero-roughness transition and the remaining terms are defined in figure 9. The displacement thickness at the element δ_k^* is taken to be the theoretical laminar value as given by reference 15.

The data of figure 8 are presented in figure 12 in terms of the dependent and independent variables of the correlating equation (2). These results indicate that the general trend of the low-speed correlation of reference 6 is preserved, but that the relative roughness size k/δ_k^* required to produce a given relative displacement $x_t/x_{t,0}$ of the transition point is increased considerably. Some differences in the detailed variation of the parameters deserve notice, however.

In figure 12(a), for example, a different behavior for each position of the 0.005-inch wire is indicated. As the wire is moved forward, it becomes less effective in promoting transition. This behavior is partially the result of the theoretical laminar boundary layer being substantially thinner than the experimental at locations near the leading edge, resulting in values of k/δ_k^* lower than theoretical. This thickening of the laminar boundary layer near the leading edge was reported in reference 3 and was rather extensively investigated in reference 18. In both cases it was associated with the degree of bluntness of the leading edge. Additional evidence of such an effect is apparent in the remaining figures where the experimental curves tend to shift toward the right as the element is placed closer to the leading edge. An attempt to correlate the data for the 0.052-inch element by using the best available estimate of the experimental displacement thickness in the roughness parameter resulted in only a partial improvement in the alinement of the results of figure 12(e). This behavior suggests that additional factors are influencing the effectiveness of the roughness elements.

Another anomaly in the results is the initial hump at the left of some of the experimental curves. This may be noted in figures 12(c), (d), and (e). The peak in these curves occurs at $u_\infty/\nu \sim 2.0\times10^5$ per inch, which is the value at which the inflection point occurred in figures 6 and 8. This may be considered as a value of u_∞/ν at which the transition location was particularly stable with respect to roughness disturbances.

A third trend in the results which bears explanation is the rise in $Re_t/Re_{t,0}$ at the right-hand extremity of all the curves of figures 12(e) and (f) and some of the curves of figures 12(c) and (d). This portion

of the curves corresponds to transition being established at the element as was pointed out in the low-speed results of reference 6. Some of these curves rise to a value of $Re_t/Re_{t,0}$ equal to unity, which means that the element is in a fully turbulent region and has no further effect on the transition-point location.

This discussion of figure 12 has indicated that, while there are some detailed trends present which are unexplained by the correlation of reference 6, the over-all trend is in the direction of the low-speed results. Figure 13 shows the approximate area into which the results of figure 12 fall. The right-side branches (fig. 12) where transition was fixed at the element or where the element was in a turbulent region have been omitted in preparing this figure. Included for comparison in figure 13 is the curve of reference 6 obtained for low-speed flows. Comparison of the high- and low-speed results indicates that a roughness parameter k/δ_k^* three to seven times as large as for the low-speed case is required to produce a given value of the transition Reynolds number ratio at Mach 3.12 for the particular cylinder model tested. The spread in the high-speed data of figure 13 seems to indicate that, while k/δ_k^* is the primary independent variable, additional parameters appear to be necessary to correlate the data into a single curve.

SUMMARY OF RESULTS

Surface-temperature measurements and high-speed schlieren photographs were used to study transition on a cylindrical model alined parallel to the air stream. The model was tested in a supersonic wind tunnel at Mach 3.12 with and without single roughness elements. The main results of the study may be summarized as follows:

1. The mean location of the transition point observed in the schlieren photographs corresponded to the location of the maximum temperature on the model surface. The temperature rise leading to the maximum surface temperature was more gradual for the cylinder than for a 10° included-angle cone.

2. The Reynolds number of transition for zero roughness was found to increase with increases in test-section Reynolds number per inch according to the equation

$$Re_t = C\sqrt{u_\infty/\nu}$$

where u_∞/ν is the Reynolds number per inch and C is a numerical constant. This expression was also found to agree approximately with certain previously published results in which the stream Mach number was varied; consequently it appears that the transition Reynolds number may be more significantly influenced by tunnel Reynolds number than by tunnel Mach number.

3. Of all the low-speed criteria used to predict the effect of single roughness elements, only Dryden's low-speed correlation parameter predicts a trend which is consistent with the present results. For the present experiment, however, Dryden's roughness parameter k/δ_k^* must be increased three to seven times to obtain a transition Reynolds number ratio equivalent to that found at low speeds. The spread in the results suggests that parameters in addition to k/δ_k^* are necessary to obtain a single-curve correlation.

Lewis Flight Propulsion Laboratory
    National Advisory Committee for Aeronautics
        Cleveland, Ohio, September 28, 1954

REFERENCES

1. Ross, Albert O.: Determination of Boundary-Layer Transition Reynolds Numbers by Surface-Temperature Measurement of a 10° Cone in Various NACA Supersonic Wind Tunnels. NACA TN 3020, 1953.

2. Evvard, J. C., Tucker, M., and Burgess, W. C., Jr.: Statistical Study of Transition-Point Fluctuations in Supersonic Flow. NACA TN 3100, 1954.

3. Brinich, Paul F., and Diaconis, Nick S.: Boundary-Layer Development and Skin Friction at Mach Number 3.05. NACA TN 2742, 1952.

4. Fage, A.: The Smallest Size of a Spanwise Surface Corrugation which Affects Boundary-Layer Transition on an Airfoil. R. & M. No. 2120, British A.R.C., 1943.

5. Fage, A., and Preston, J. H.: On Transition from Laminar to Turbulent Flow in the Boundary Layer. Proc. Royal Soc. (London), ser. A, vol. 178, June 12, 1941, pp. 201-227.

6. Dryden, Hugh L.: Review of Published Data on the Effect of Roughness on Transition from Laminar to Turbulent Flow. Jour. Aero. Sci., vol. 20, no. 7, July 1953, pp. 477-482.

7. Gazley, Carl, Jr.: Boundary-Layer Stability and Transition in Subsonic and Supersonic Flow. Jour. Aero. Sci., vol. 20, no. 1, Jan. 1953, pp. 19-28.

8. Tani, I., Hama, R., and Mituisi, S.: On the Permissible Roughness in the Laminar Boundary Layer. Rep. No. 99, Aero. Res. Inst., Tokyo Imperial Univ., vol. 15, no. 13, Oct. 1940, pp. 417-428.

3273

NACA TN 3267   17

9. Tani, Itiro, and Hama, Francis R.: Some Experiments on the Effect of a Single Roughness Element on Boundary-Layer Transition. Jour. Aero. Sci., vol. 20, no. 4, Apr. 1953, pp. 289-290.

10. Low, George M.: Cooling Requirements for Stability of Laminar Boundary Layer with Small Pressure Gradients at Supersonic Speeds. NACA TN 3103, 1954.

11. Ribner, H. S., and Tucker, M.: Spectrum of Turbulence in a Contracting Stream. NACA Rep. 1113, 1953. (Supersedes NACA TN 2606.)

12. Tucker, Maurice, and Maslen, Stephen H.: Turbulent Boundary-Layer Temperature Recovery Factors in Two-Dimensional Supersonic Flow. NACA TN 2296, 1951.

13. Taylor, G. I.: Statistical Theory of Turbulence. V - Effect of Turbulence on Boundary Layer. Theoretical Discussion of Relationship Between Scale of Turbulence and Critical Resistance of Spheres. Proc. Roy. Soc. (London), ser. A, vol. 156, no. 888, Aug. 17, 1936, pp. 307-317.

14. Lee, Roland E.: Measurements of Pressure Distribution and Boundary-Layer Transition on a Hollow-Cylinder Model. NAVORD Rep. 2823, U.S. Naval Ord. Lab. (Maryland), Apr. 28, 1953.

15. Chapman, Dean R., and Rubesin, Morris W.: Temperature and Velocity Profiles in the Compressible Laminar Boundary Layer with Arbitrary Distribution of Surface Temperature. Jour. Aero. Sci., vol. 16, no. 9, Sept. 1949, pp. 547-565.

16. Czarnecki, K. R., and Sinclair, Archibald R.: Factors Affecting Transition at Supersonic Speeds. NACA RM L53I18a, 1953.

17. Dryden, Hugh L.: Effects of Roughness and Suction on Transition for Laminar to Turbulent Flows. Jublie-Scientifique De M. Dimitri Riabouchinsky's Publications Scientifique et Technique Du Ministere De L'Air, Paris, 1954, pp. 49-60.

18. Bradfield, W. S., DeCoursin, D. G., and Blumer, C. B.: The Effect of Leading Edge Bluntness on Momentum Loss Measurements in a Laminar Supersonic Boundary Layer. Rep. No. 96, Dept. Aero. Eng. Rosemount Res. Lab., Univ. of Minn., Sept. 1953.

3273

CL-3

Detail A
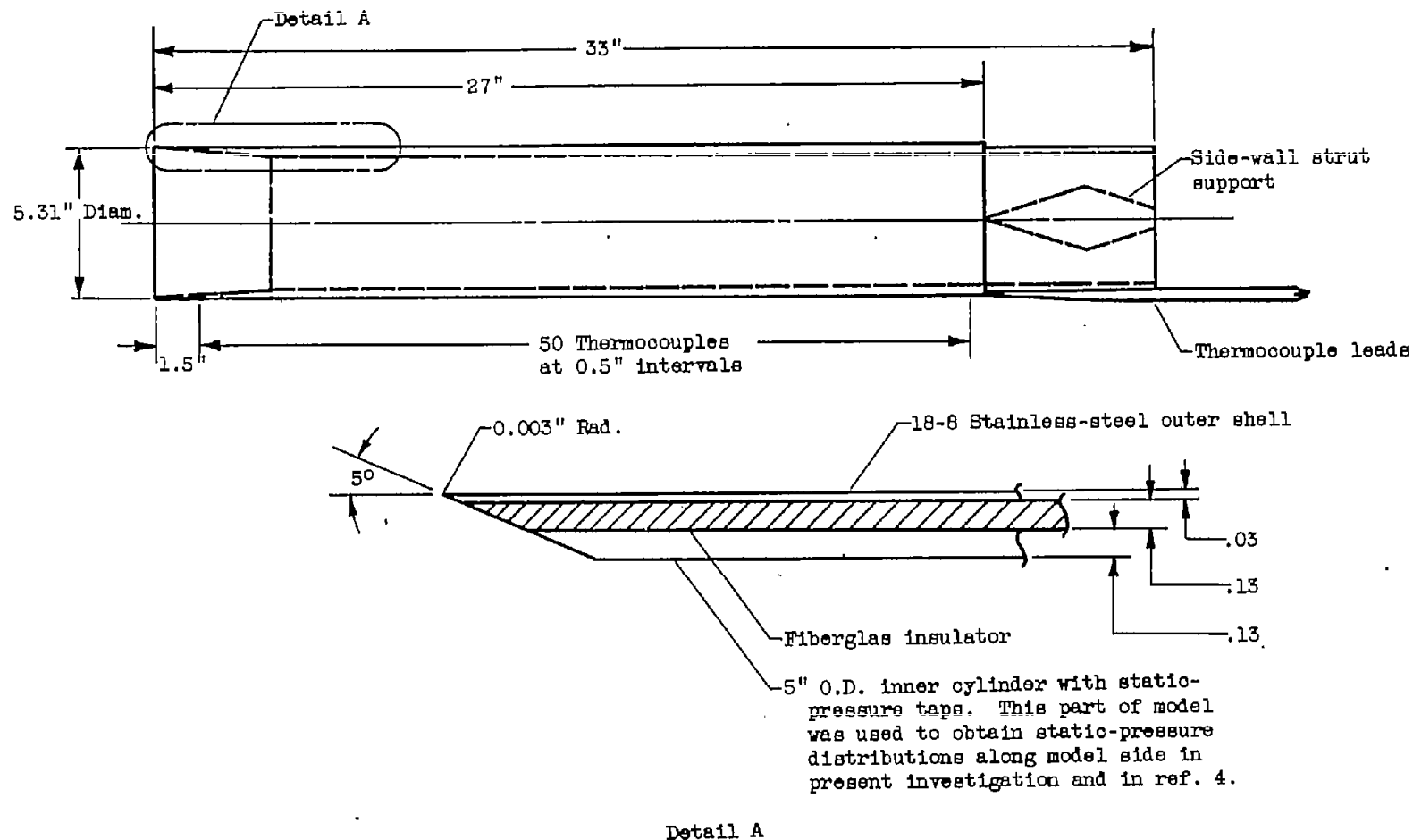
Figure 1. – Cylinder model with thermocouple instrumentation for detecting transition.
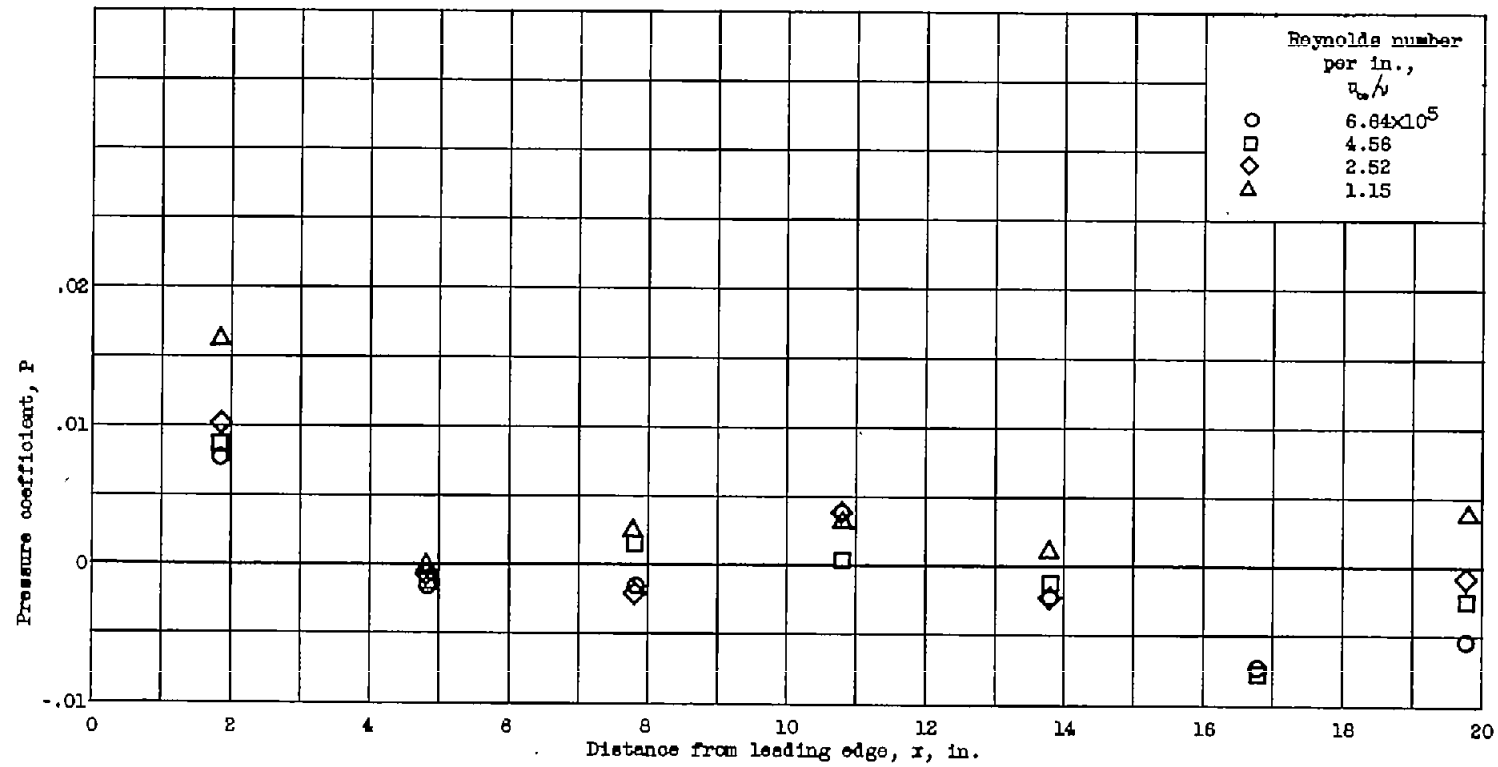
Figure 2. - Variation of pressure coefficient along cylinder (side).
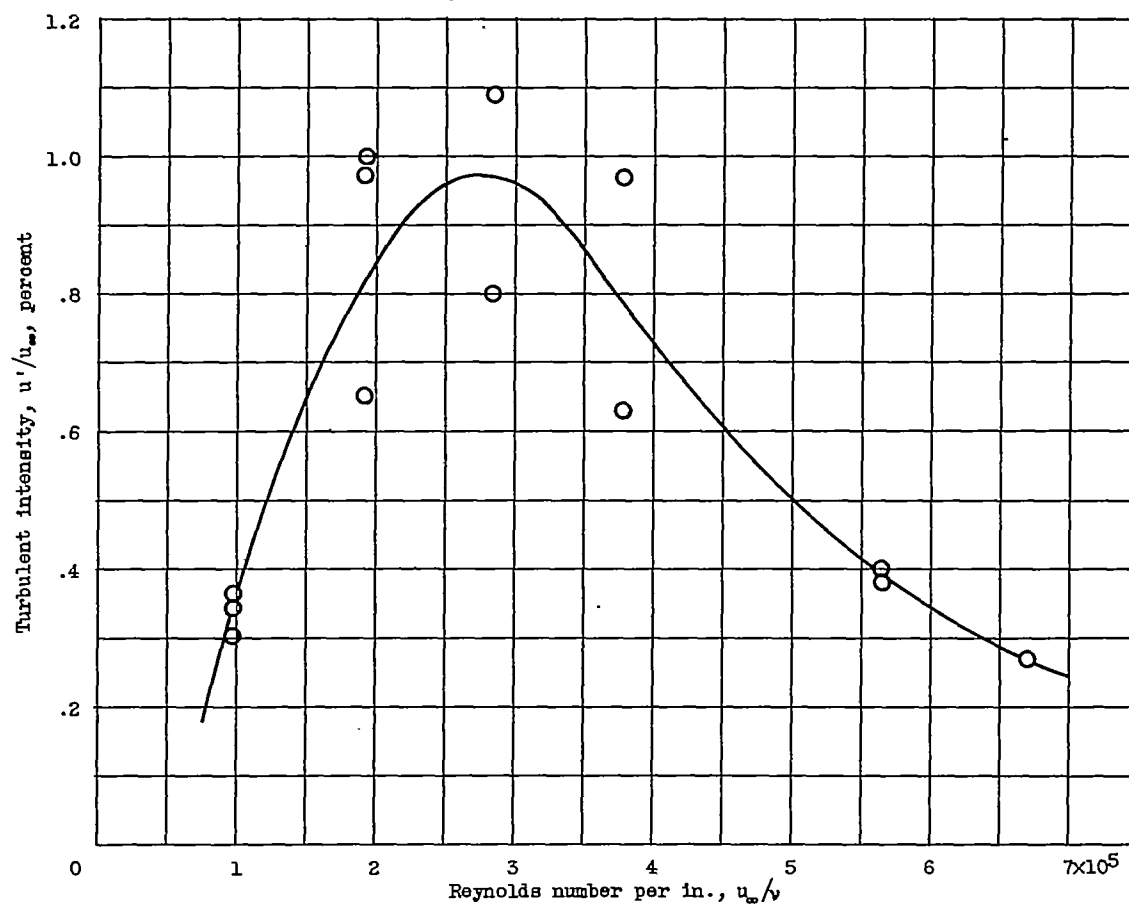
Figure 3. - Variation of turbulent intensity ahead of tunnel contraction with test-section Reynolds number.
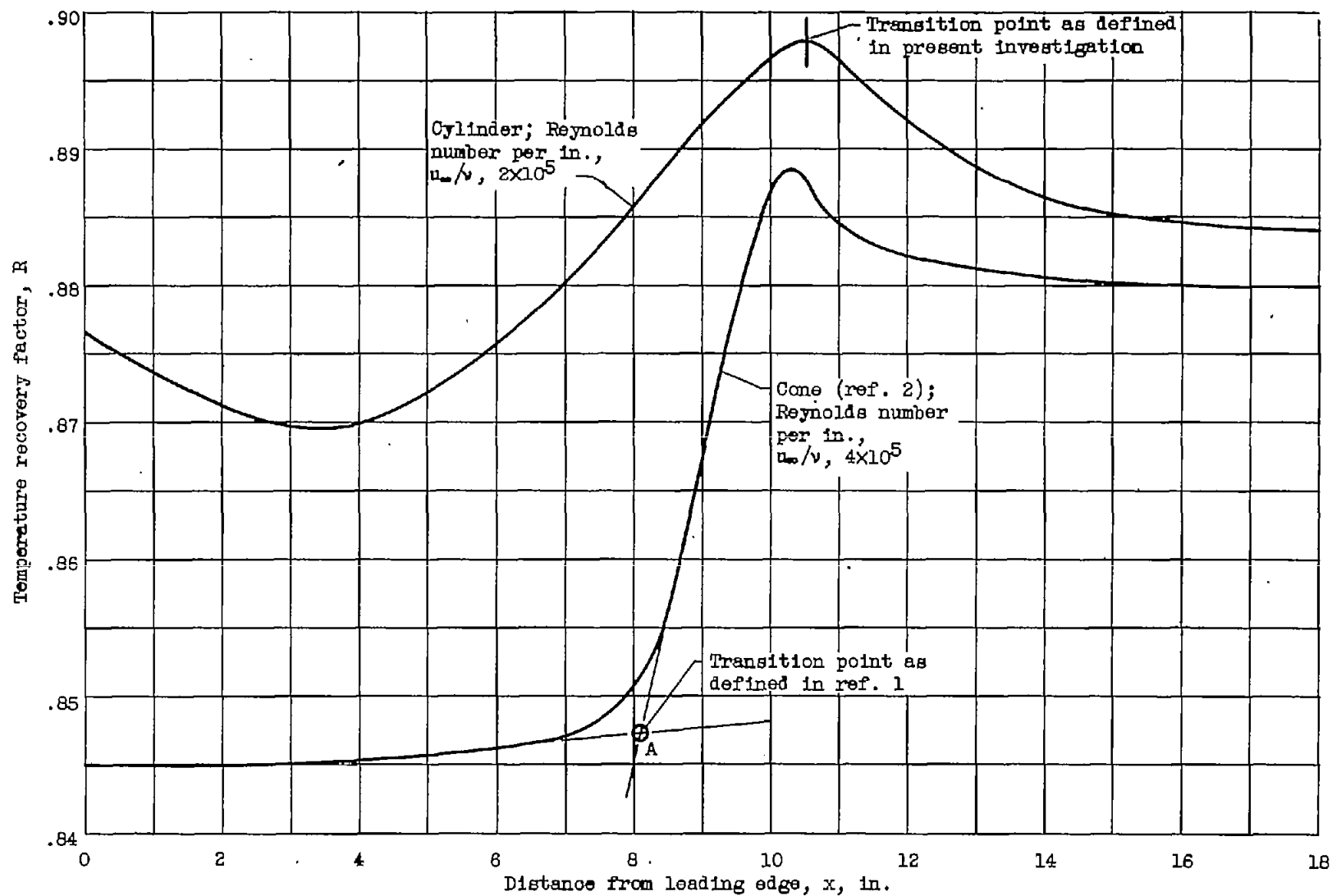
Figure 4. - Comparison of typical recovery-factor distributions on a cylinder and a cone.
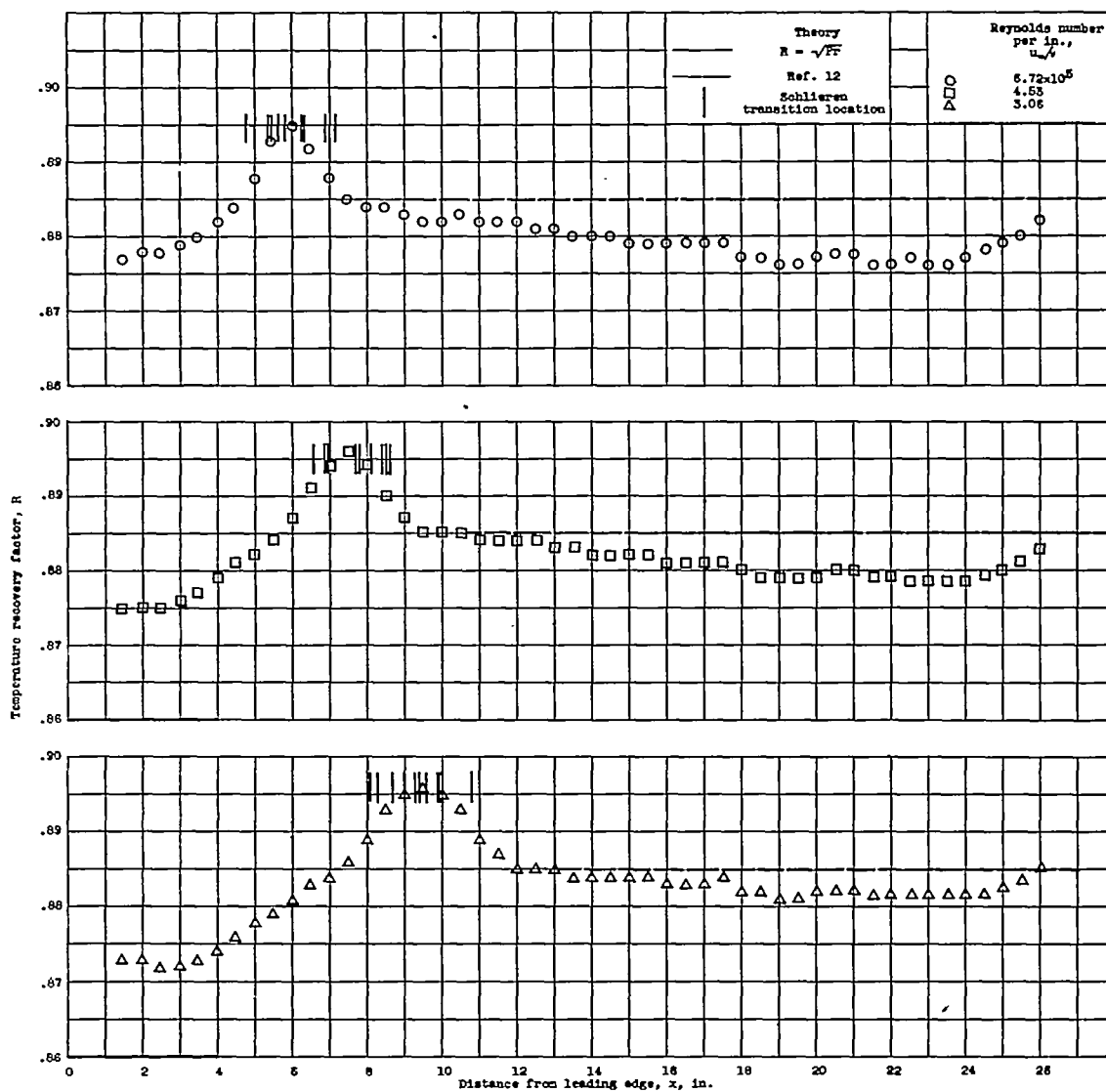
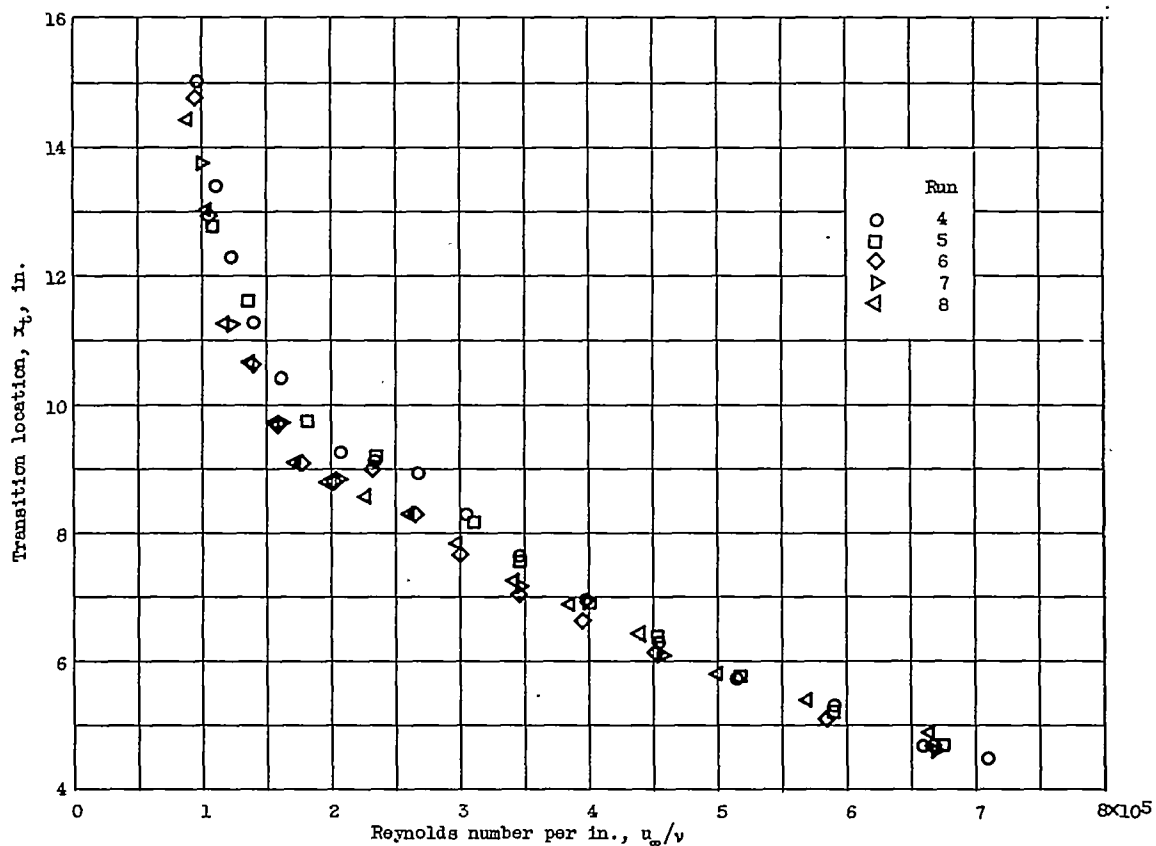Figure 5. - Effect of test-section Reynolds number on recovery-factor distribution.
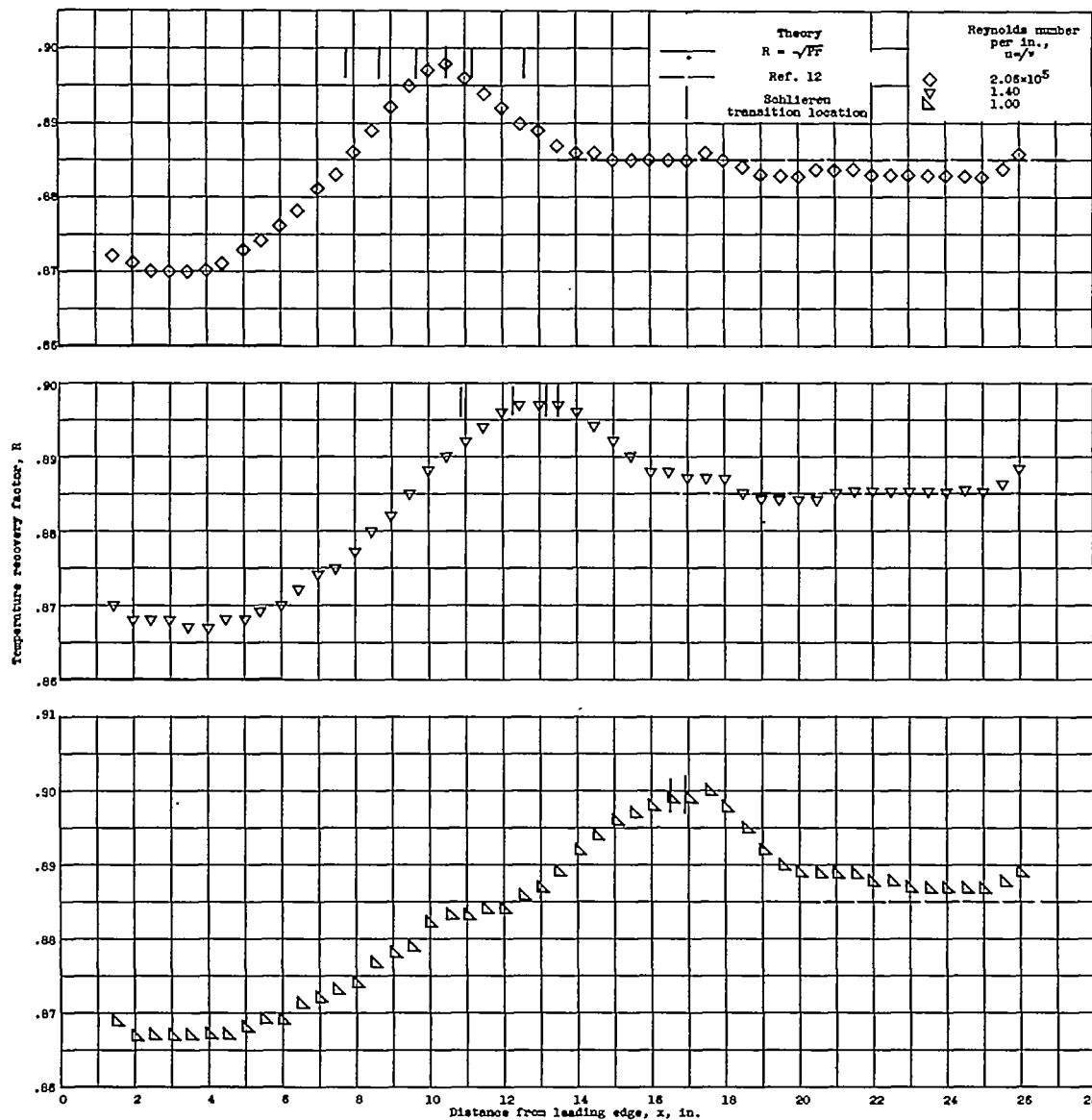
Figure 5. - Concluded. Effect of test-section Reynolds number on recovery-factor distribution.
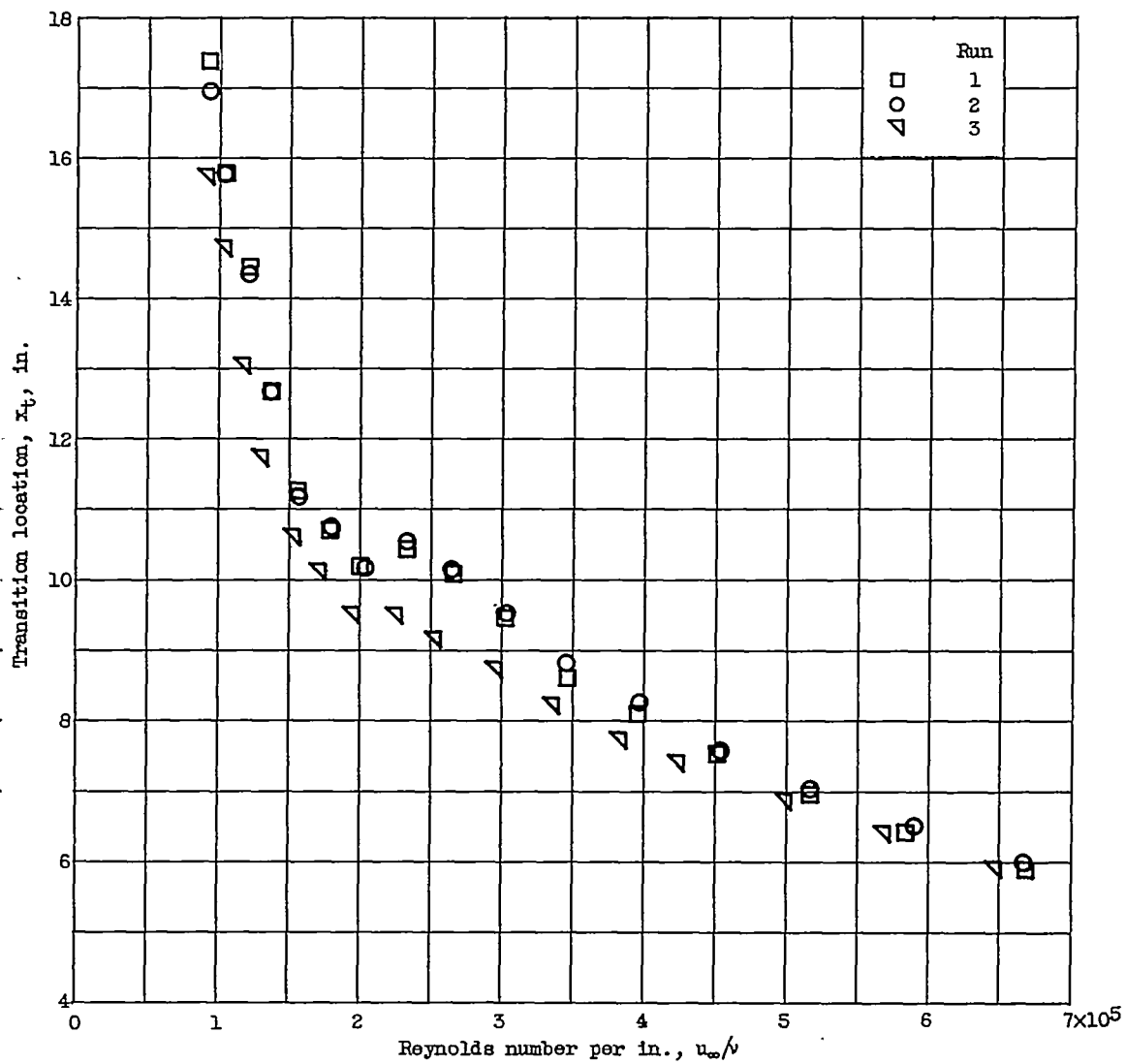
(a) Bottom of model.

Figure 6. - Effect of test-section Reynolds number on transition location.

(b) Side of model.

Figure 6. - Concluded. Effect of test-section Reynolds number on transition location.
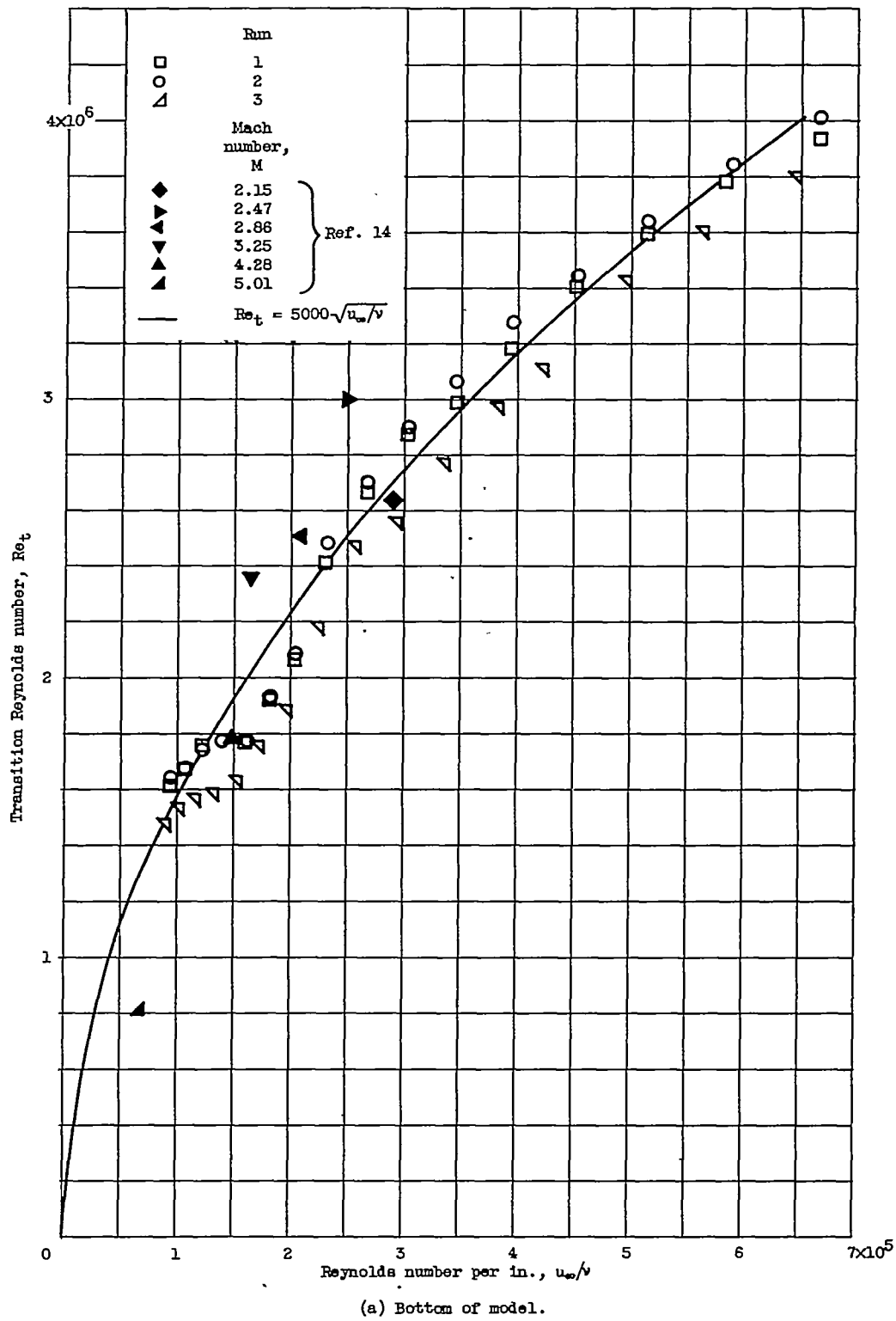
(a) Bottom of model.

Figure 7. - Transition Reynolds-number variation with test-section Reynolds number.

3273

CL-4 back

(b) Side of model.
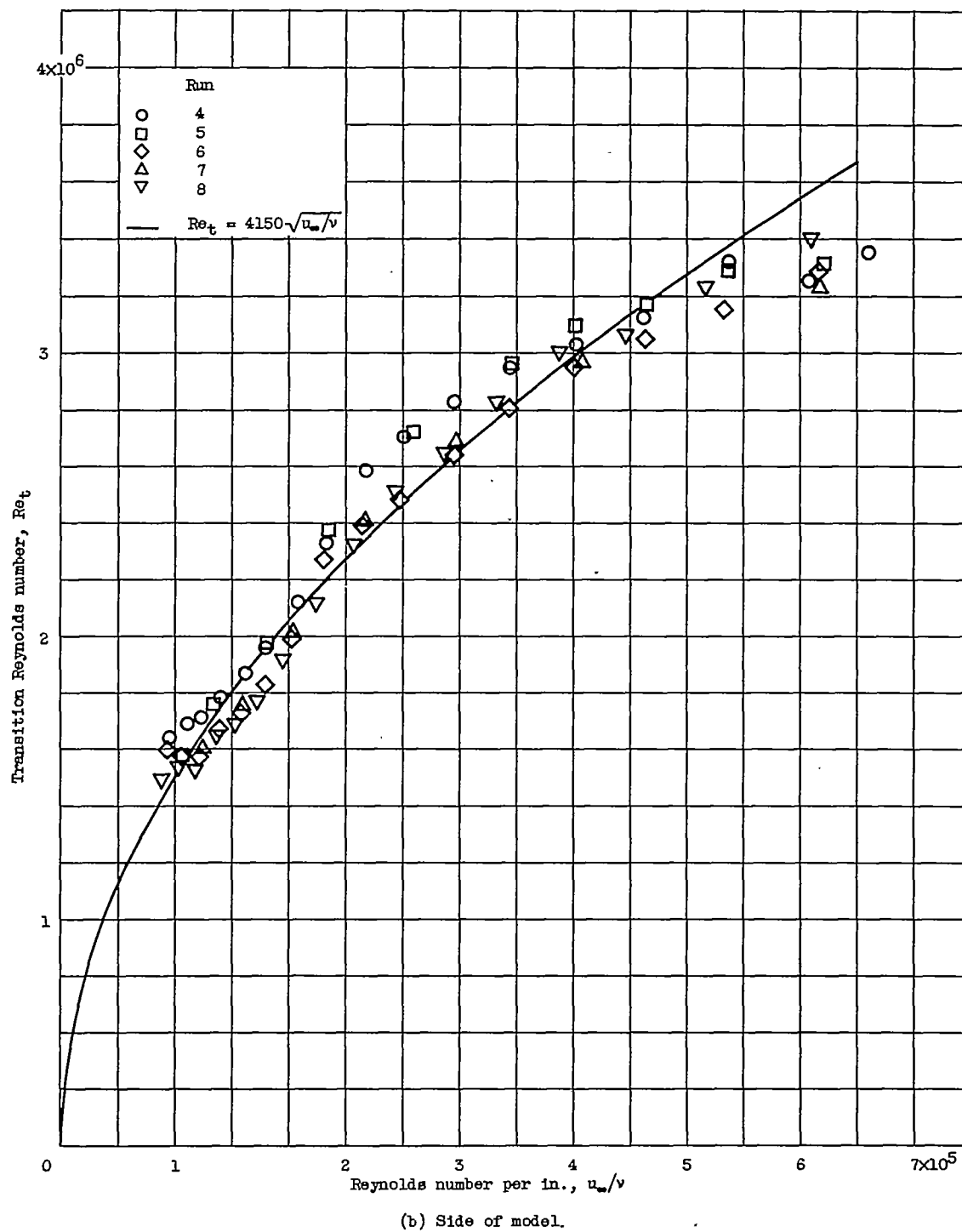
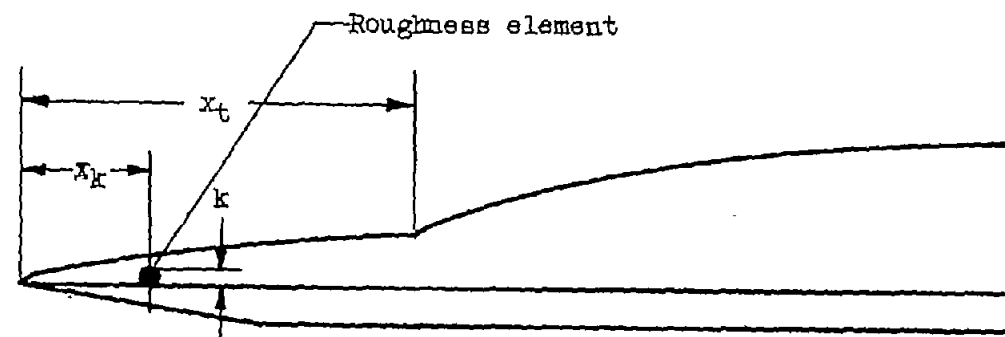Figure 7. - Concluded. Transition Reynolds number variation with test-section Reynolds number.
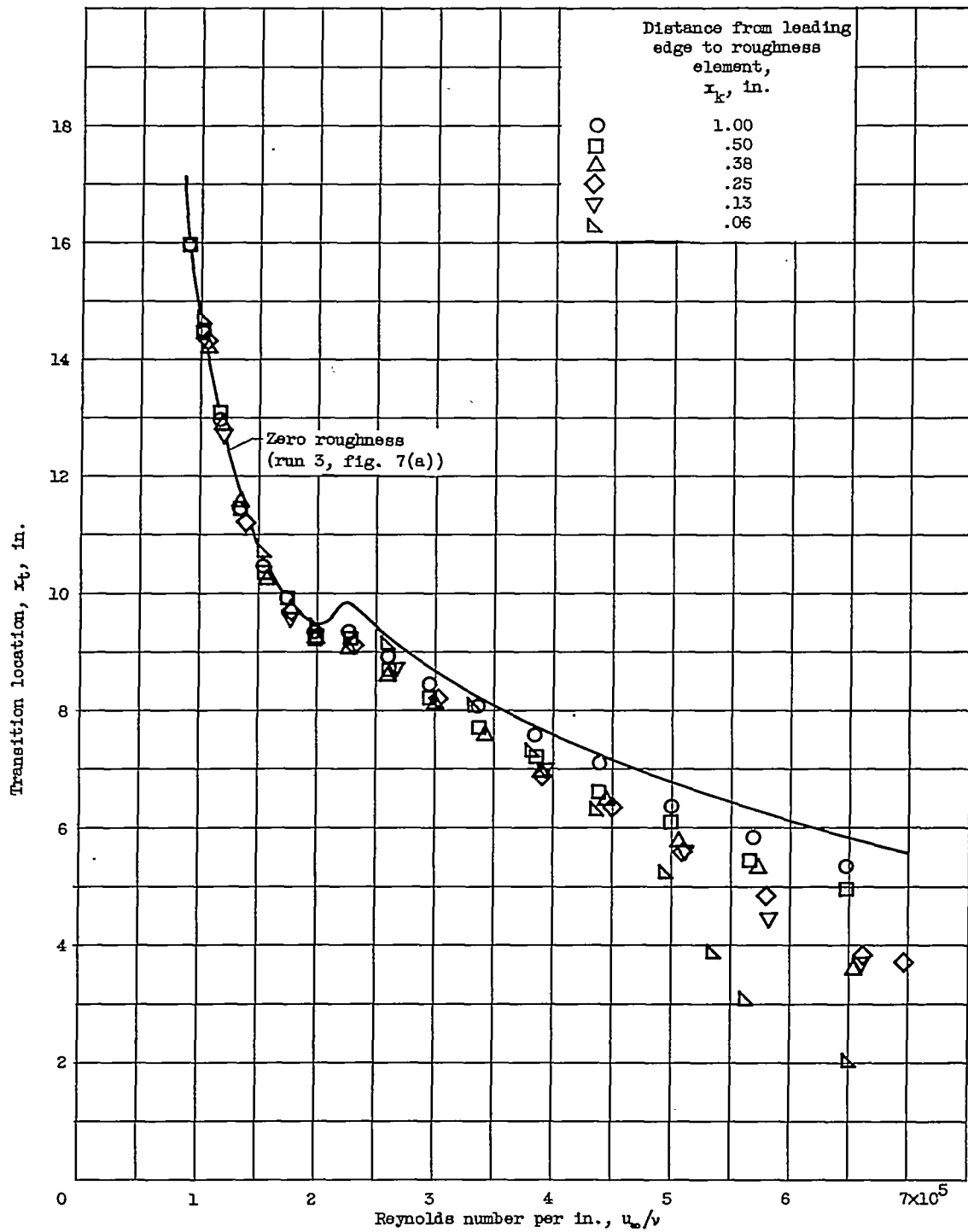
(a) Height of roughness element k, 0.005 inch; bottom of model.

Figure 8. - Effect of test-section Reynolds number and position of single roughness element on transition location.

3273
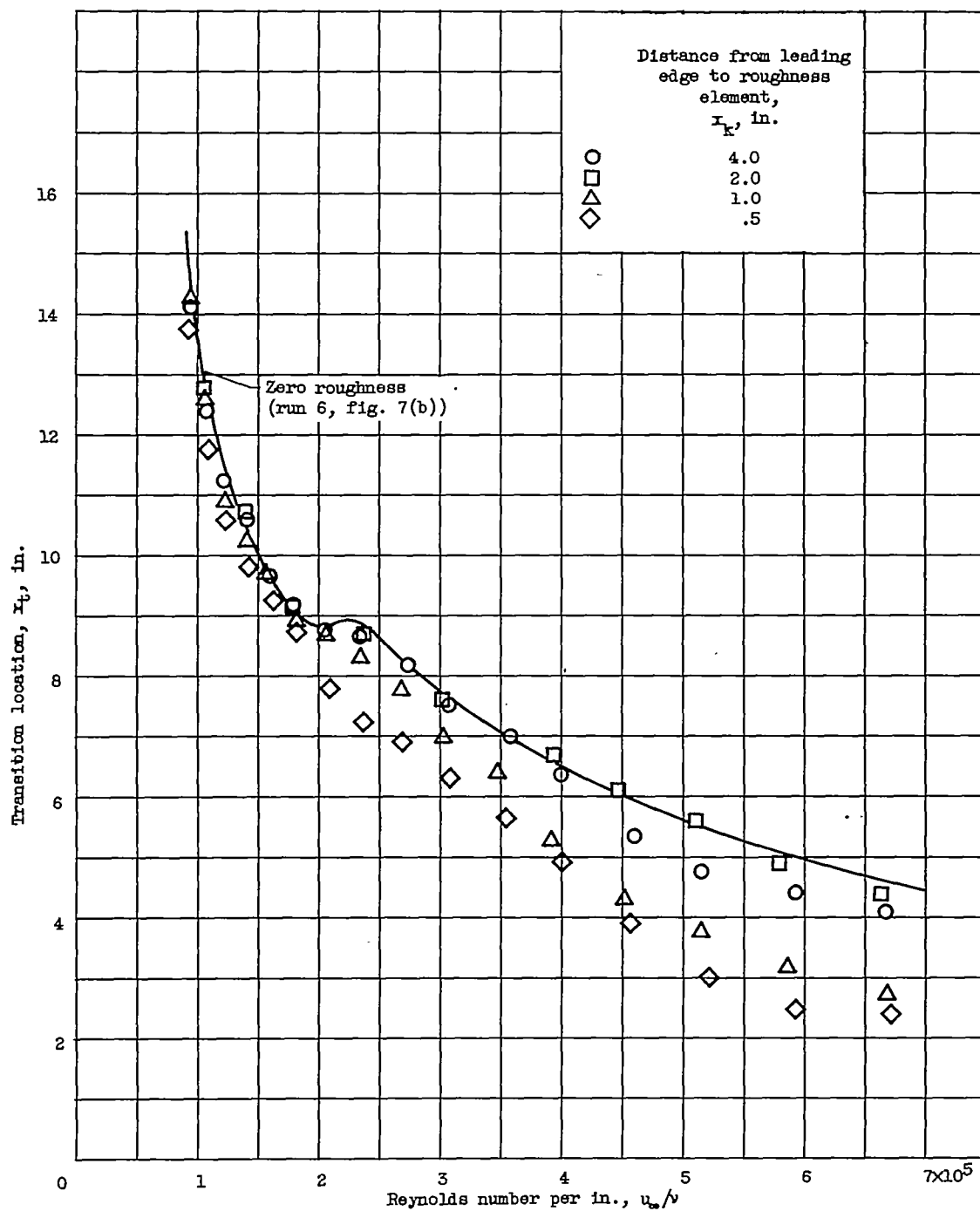
(b) Height of roughness element k, 0.010 inch; side of model.

Figure 8. - Continued. Effect of test-section Reynolds number and position of single roughness element on transition location.

(c) Height of roughness element k, 0.020 inch; side of model

Figure 8. - Continued. Effect of test-section Reynolds number and position of single roughness element on transition location.

3273
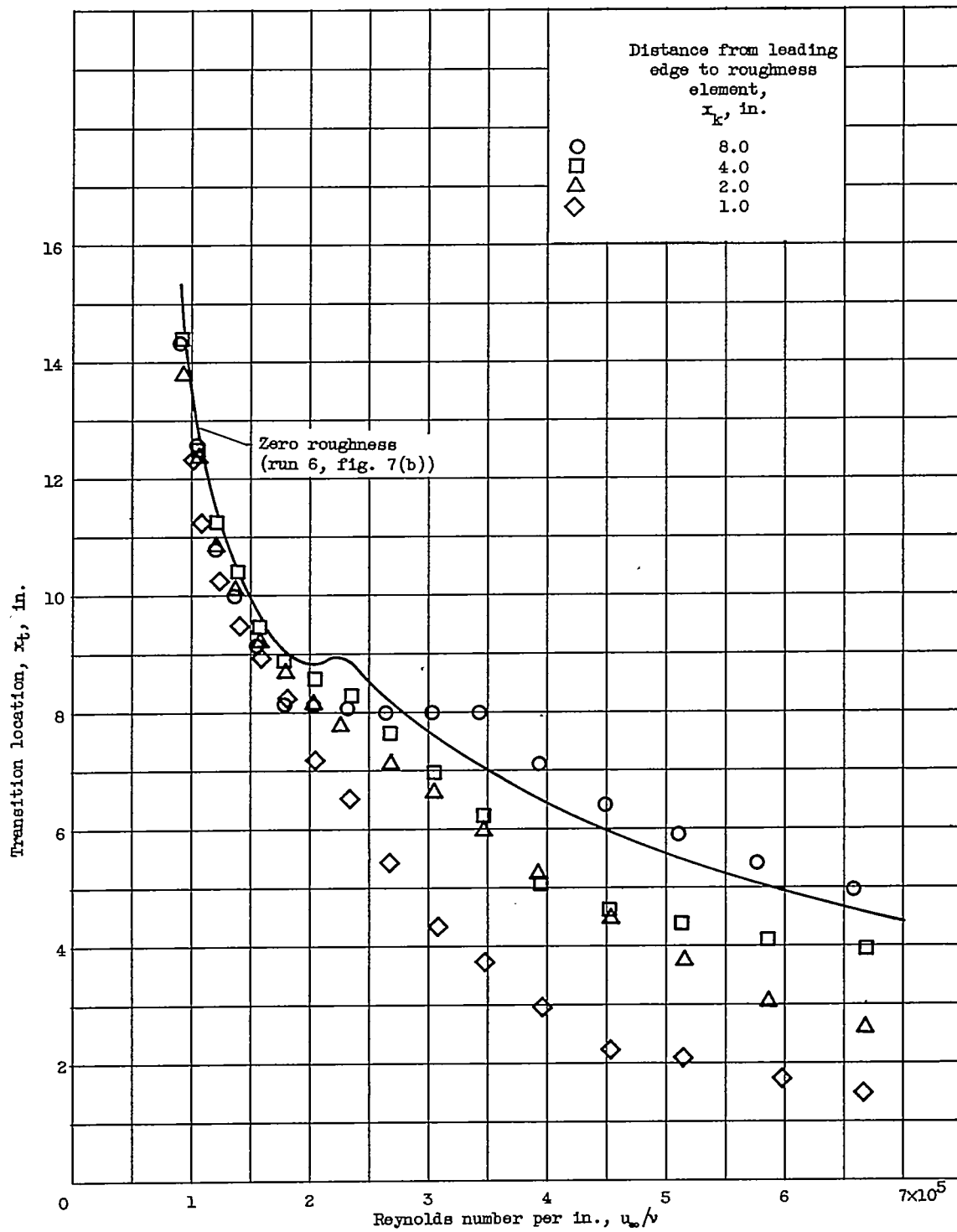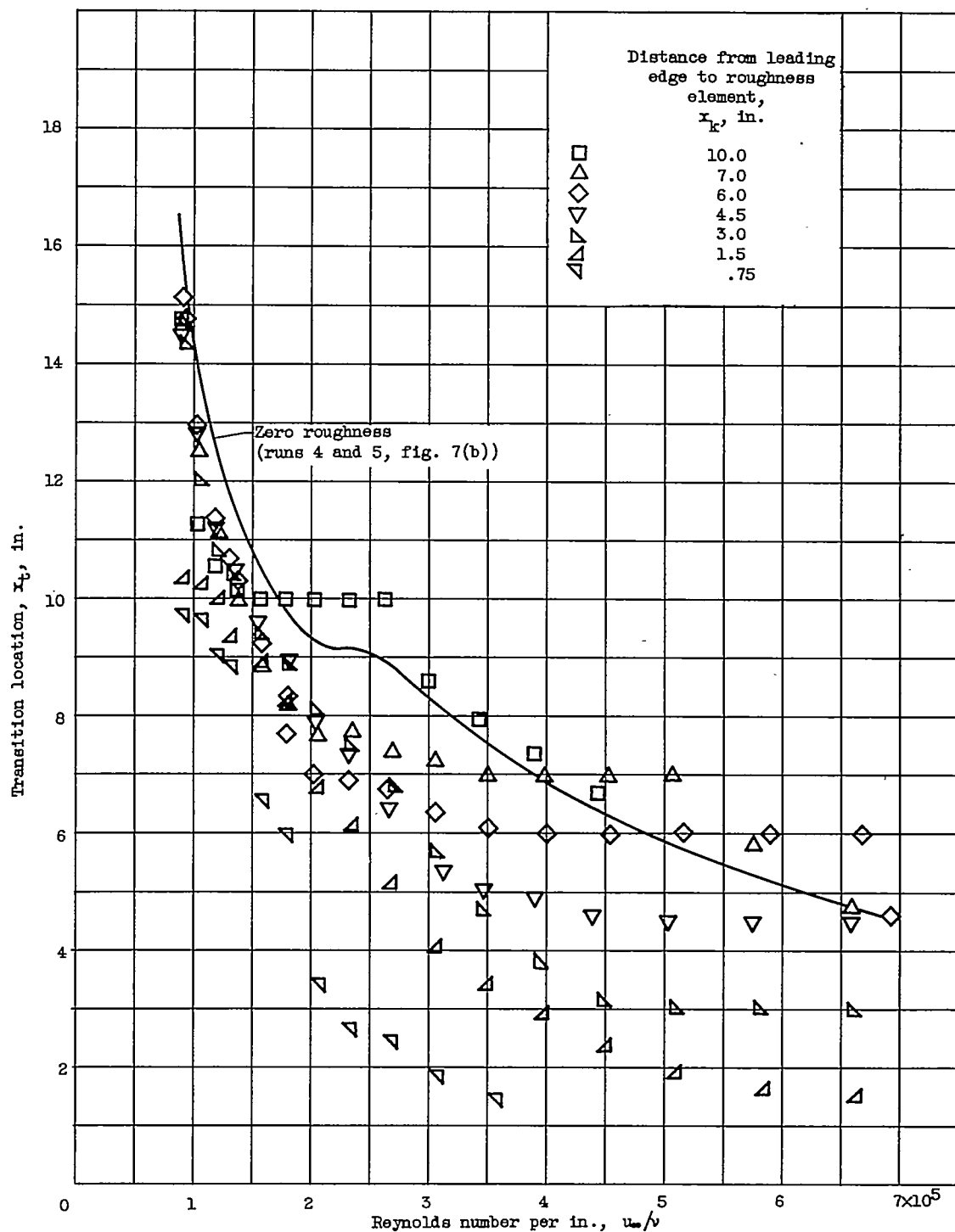
(d) Height of roughness element k, 0.032 inch; side of model.

Figure 8. - Continued. Effect of test-section Reynolds number and position of single roughness element on transition location.
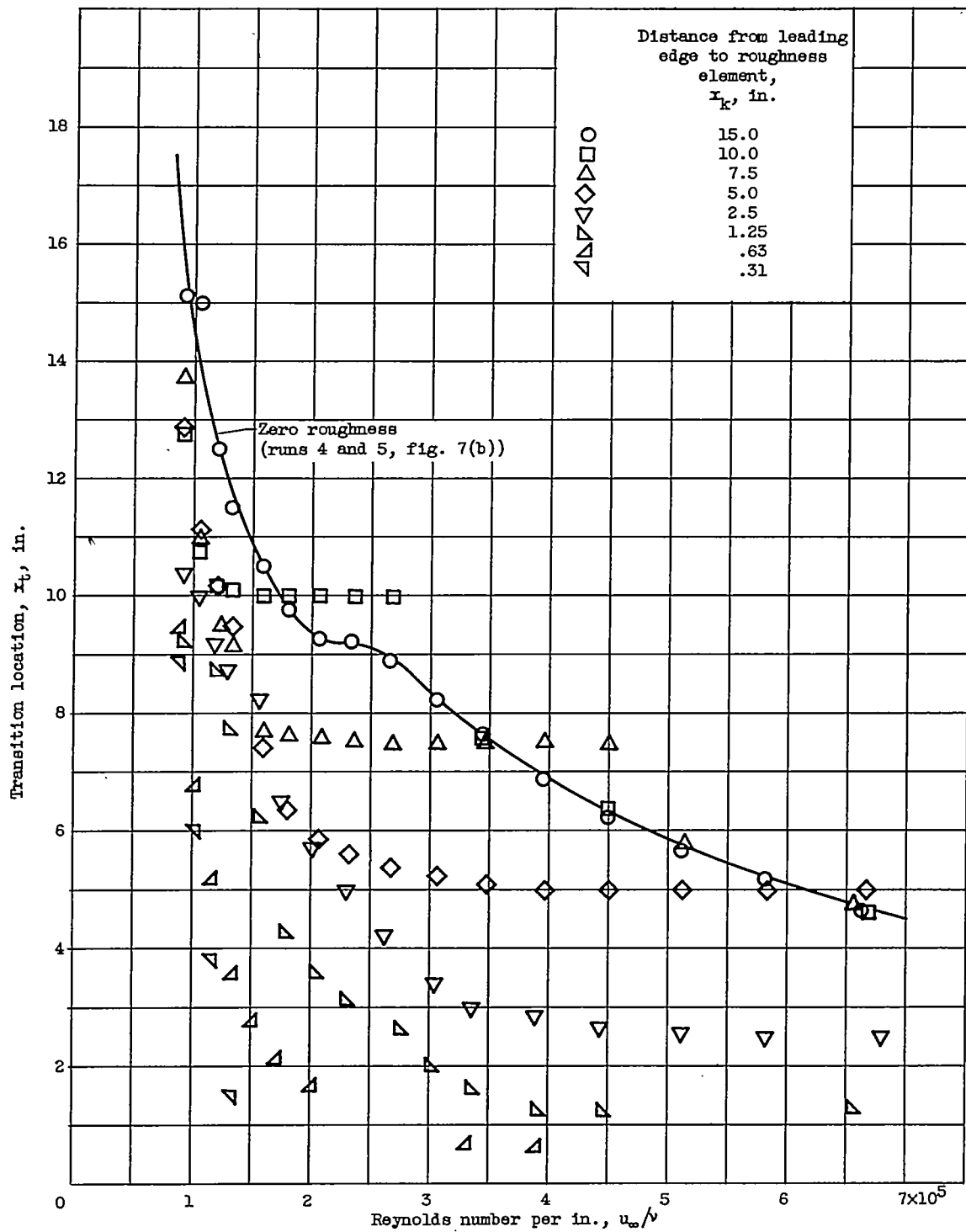
(e) Height of roughness element k, 0.052 inch; side of model.

Figure 8. - Continued. Effect of test-section Reynolds number and position of single
roughness element on transition location.
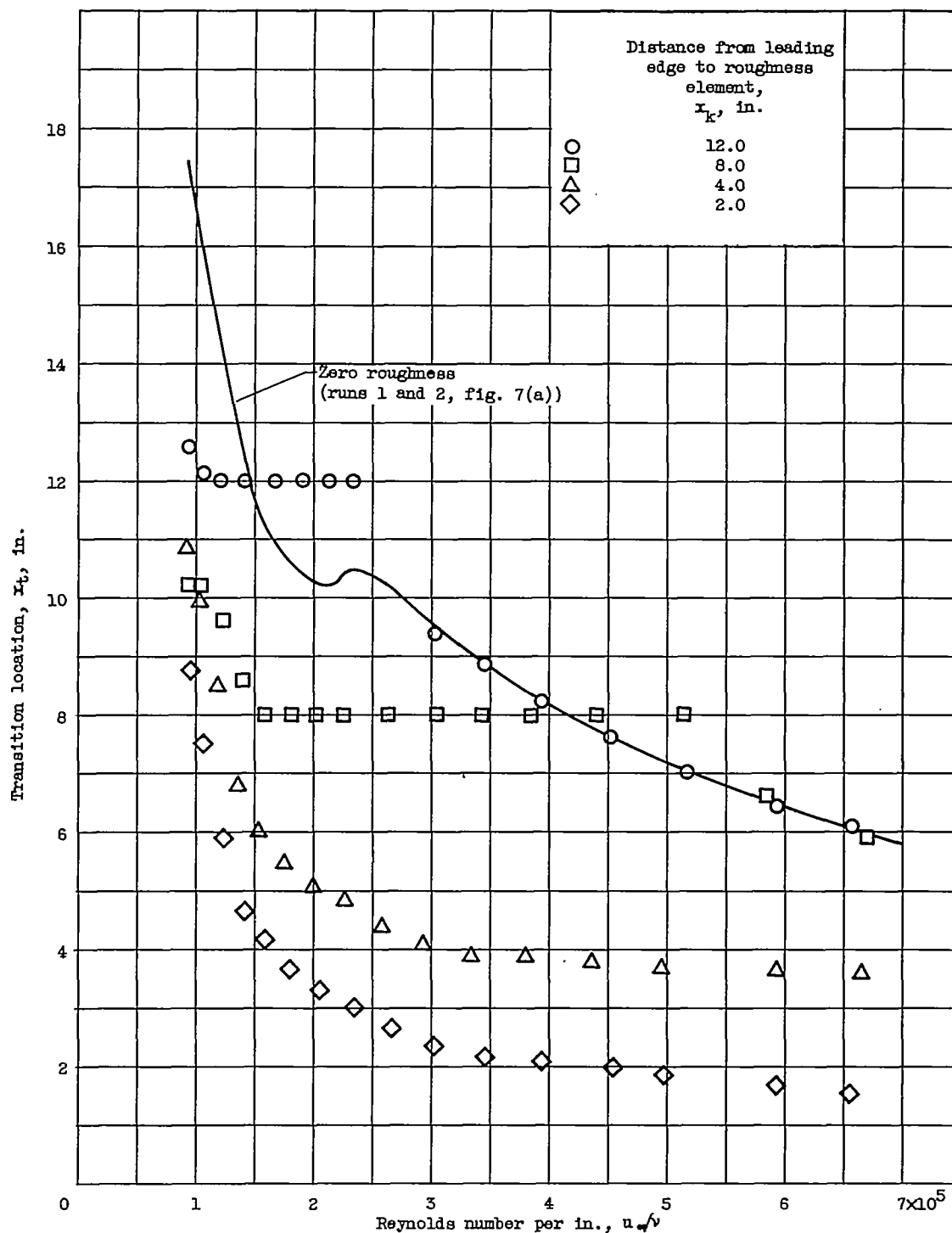
(f) Height of roughness element k, 0.079 inch; bottom of model.

Figure 8. - Concluded. Effect of test-section Reynolds number and position of single
roughness element on transition location.
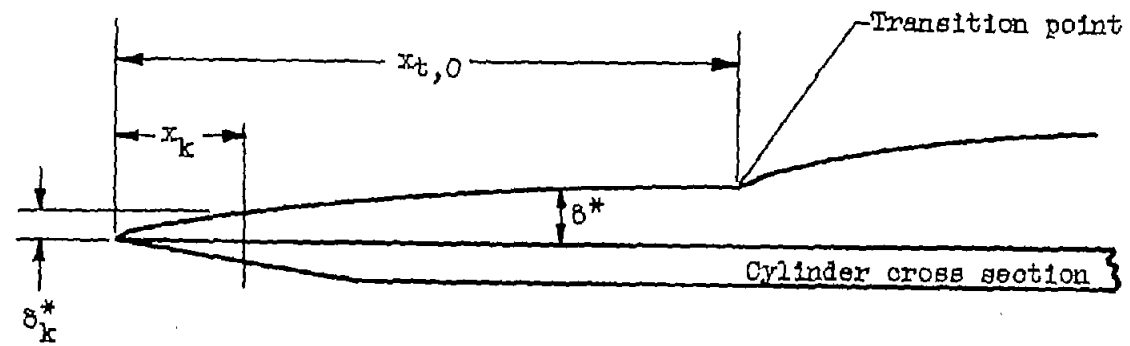
(a) Without roughness.

(b) With roughness.

Figure 9. - Schematic diagram showing quantities considered in transition analysis.
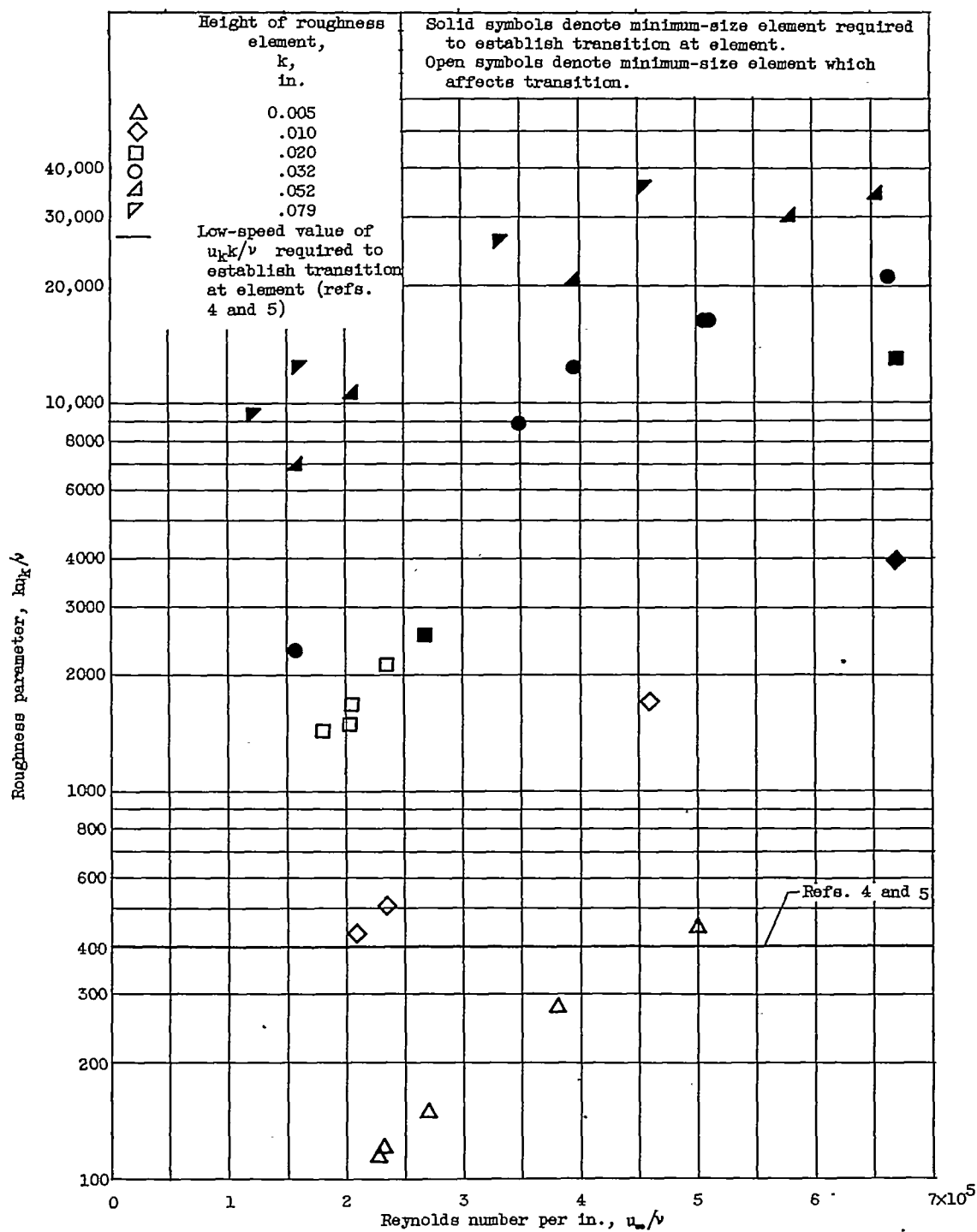
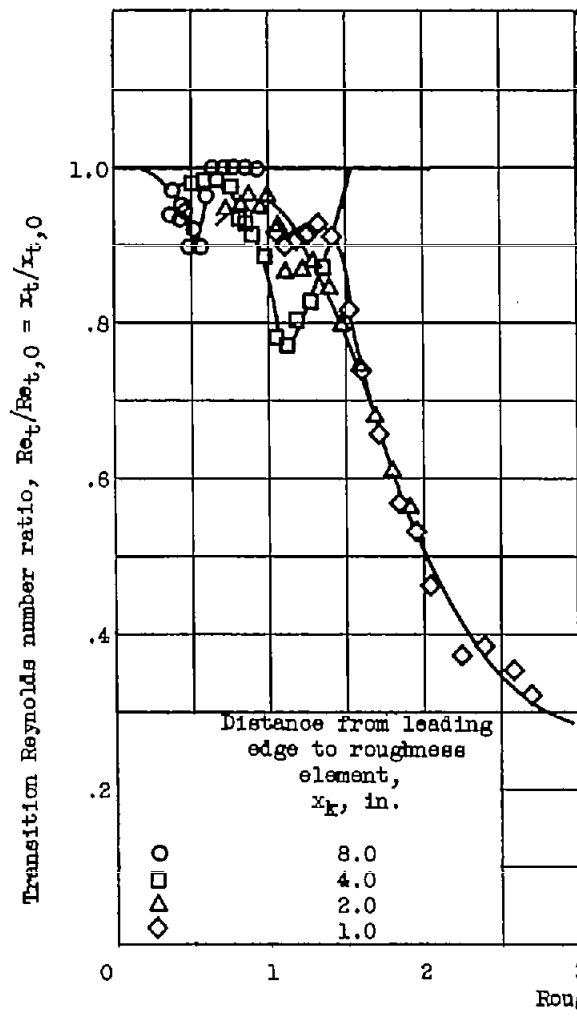Figure 10. - Effect of test-section Reynolds number and element size on transition roughness parameter ku_k/ν.
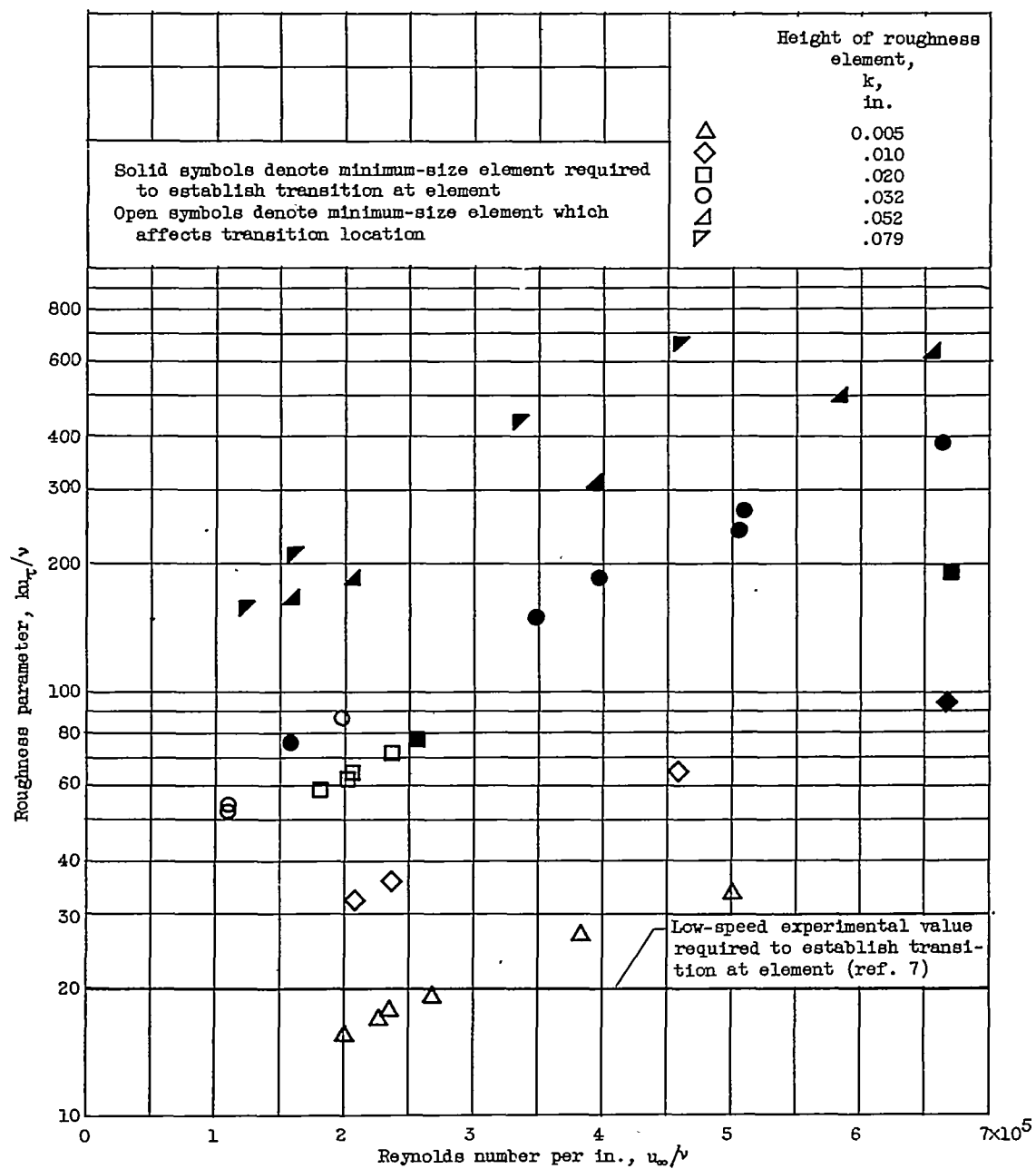
Figure 11. - Effect of test-section Reynolds number and element size on transition roughness parameter ku_τ/ν.
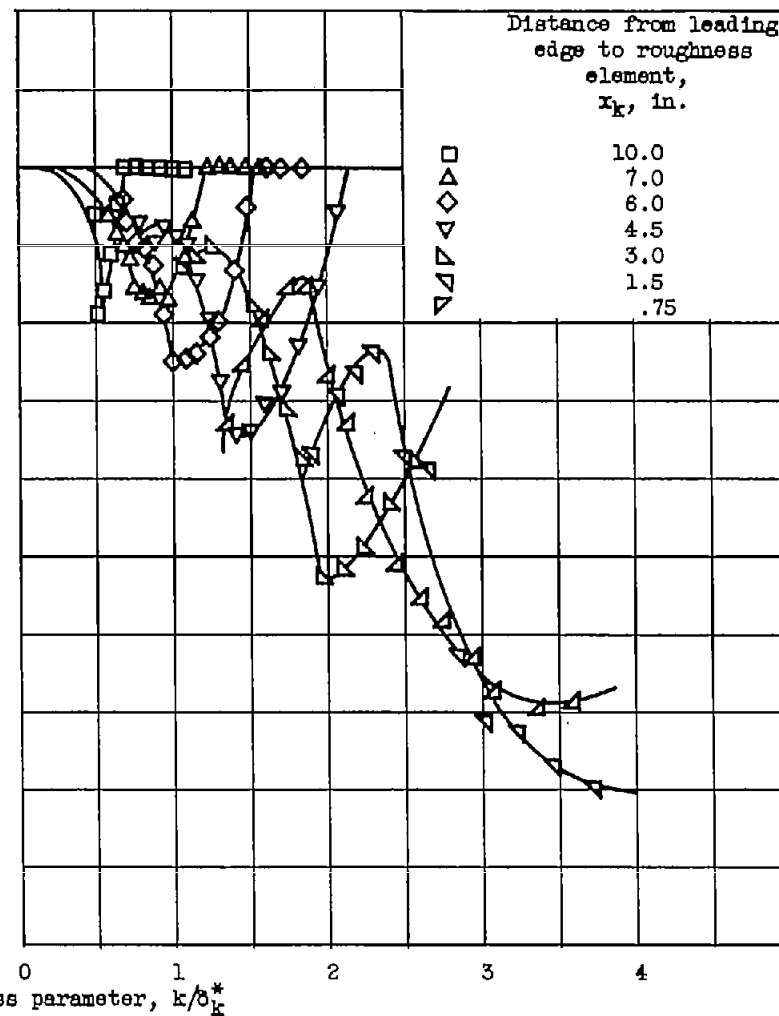
(a) Height of roughness element k, 0.005 inch.

(b) Height of roughness element k, 0.010 inch.
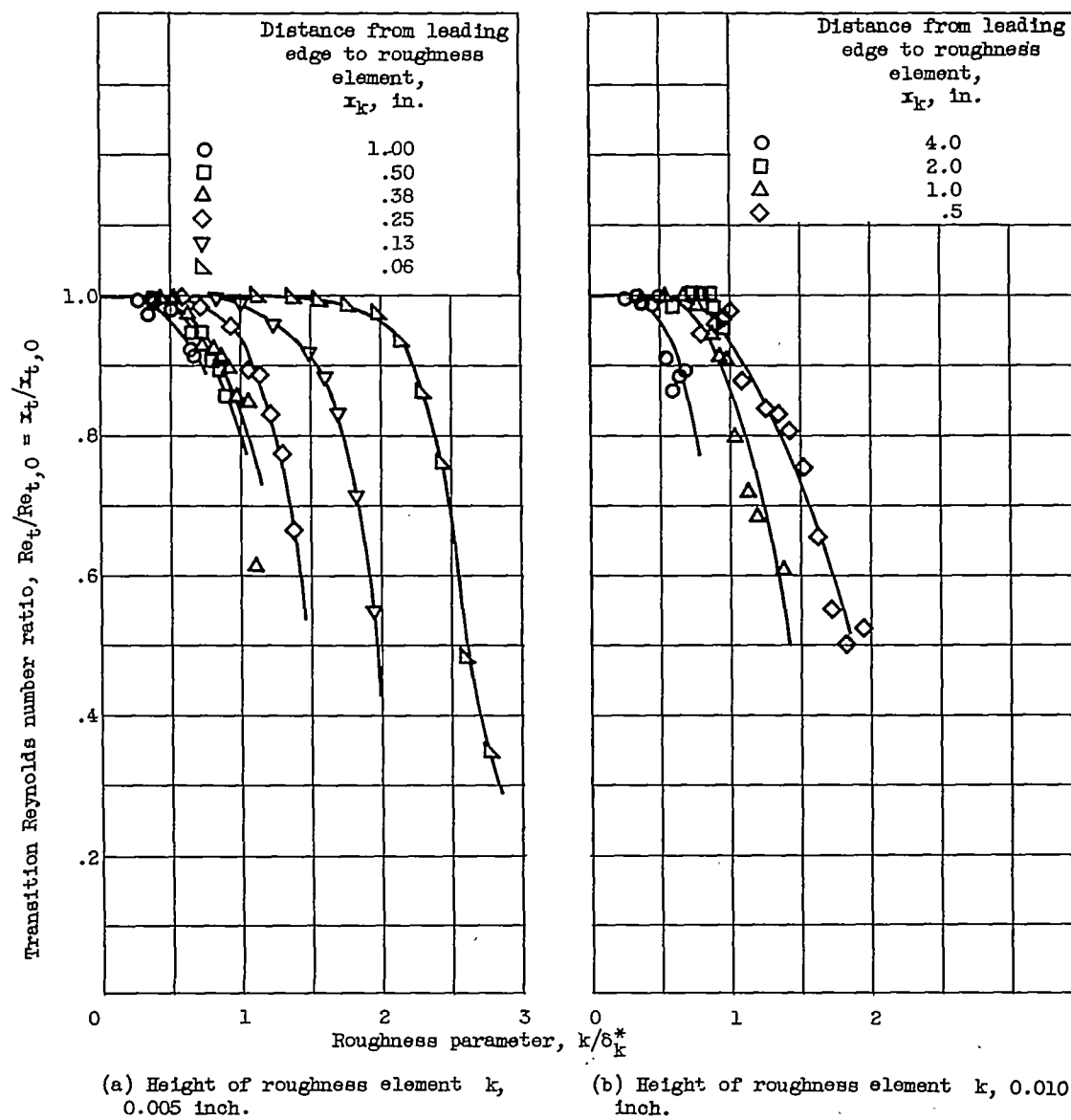
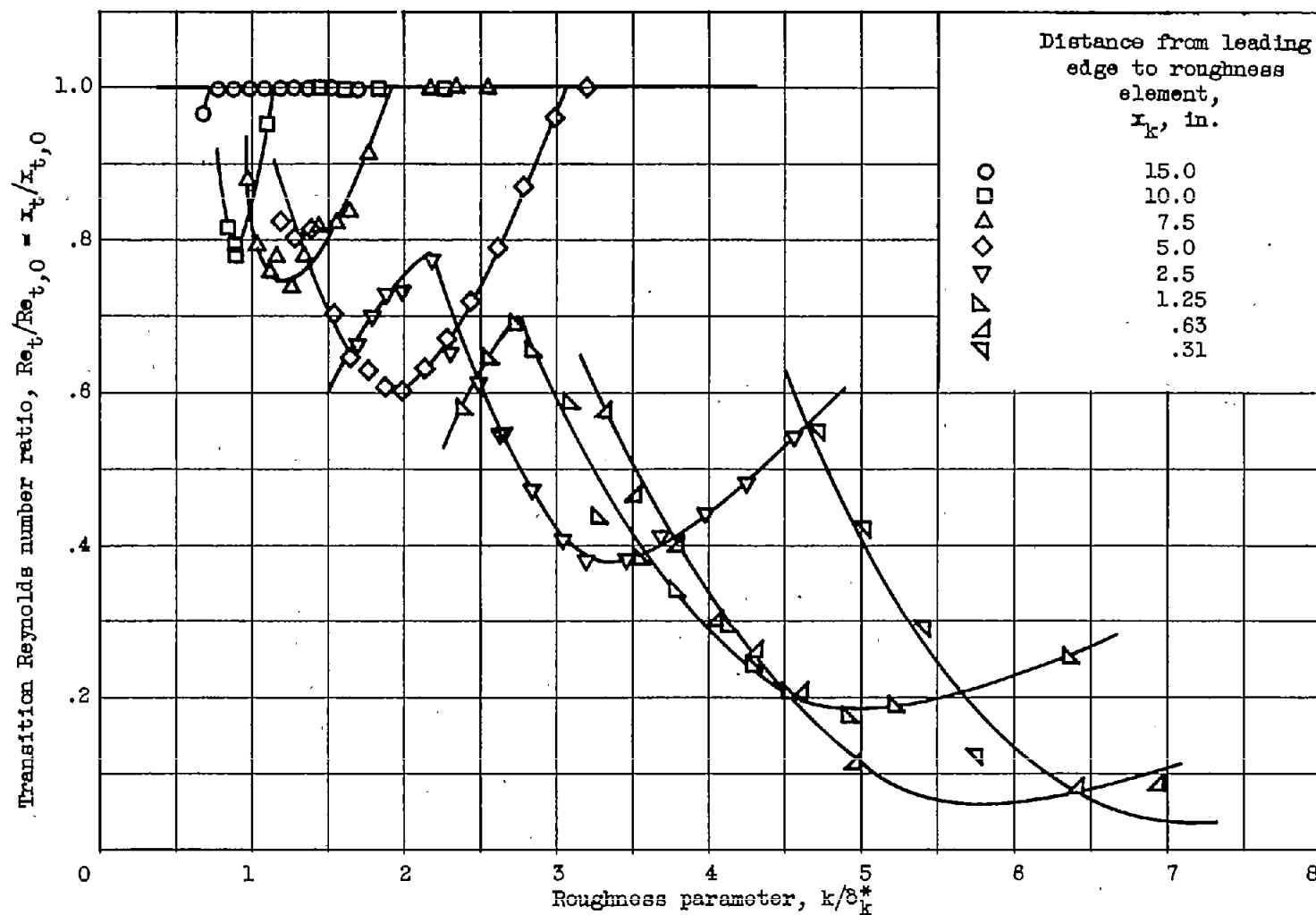Figure 12. - Effect of roughness parameter k/δ_k^* on transition Reynolds number ratio.

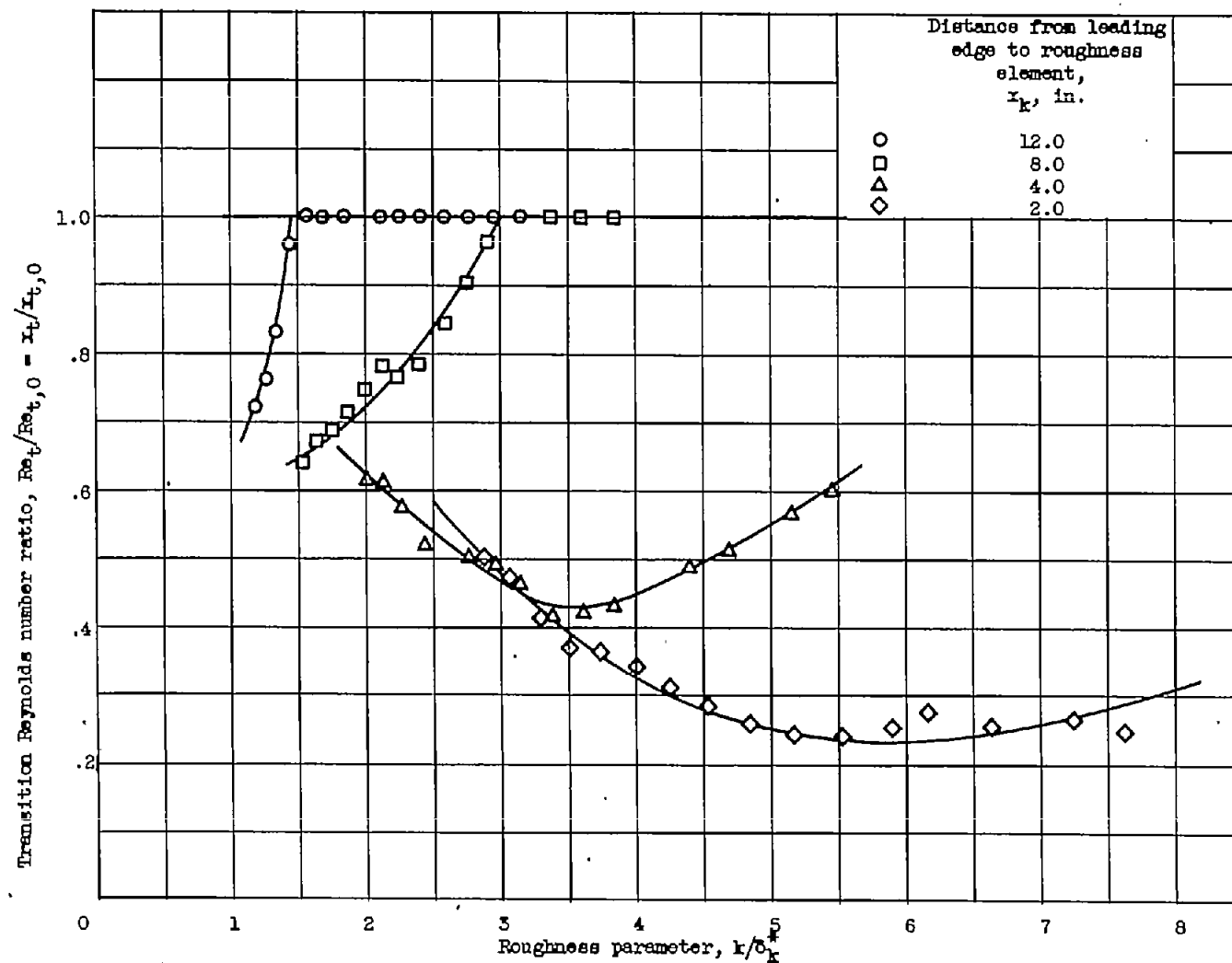(c) Height of roughness element k, 0.020 inch.

(d) Height of roughness element k, 0.032 inch.

Figure 12. - Continued. Effect of roughness parameter k/δ_k^* on transition Reynolds number ratio.

(e) Height of roughness element k, 0.052 inch.

Figure 12. - Continued. Effect of roughness parameter k/δ_k^* on transition Reynolds number ratio.

(f) Height of roughness element k, 0.079 inch.

Figure 12. - Concluded. Effect of roughness parameter k/δ_k^* on transition Reynolds number ratio.
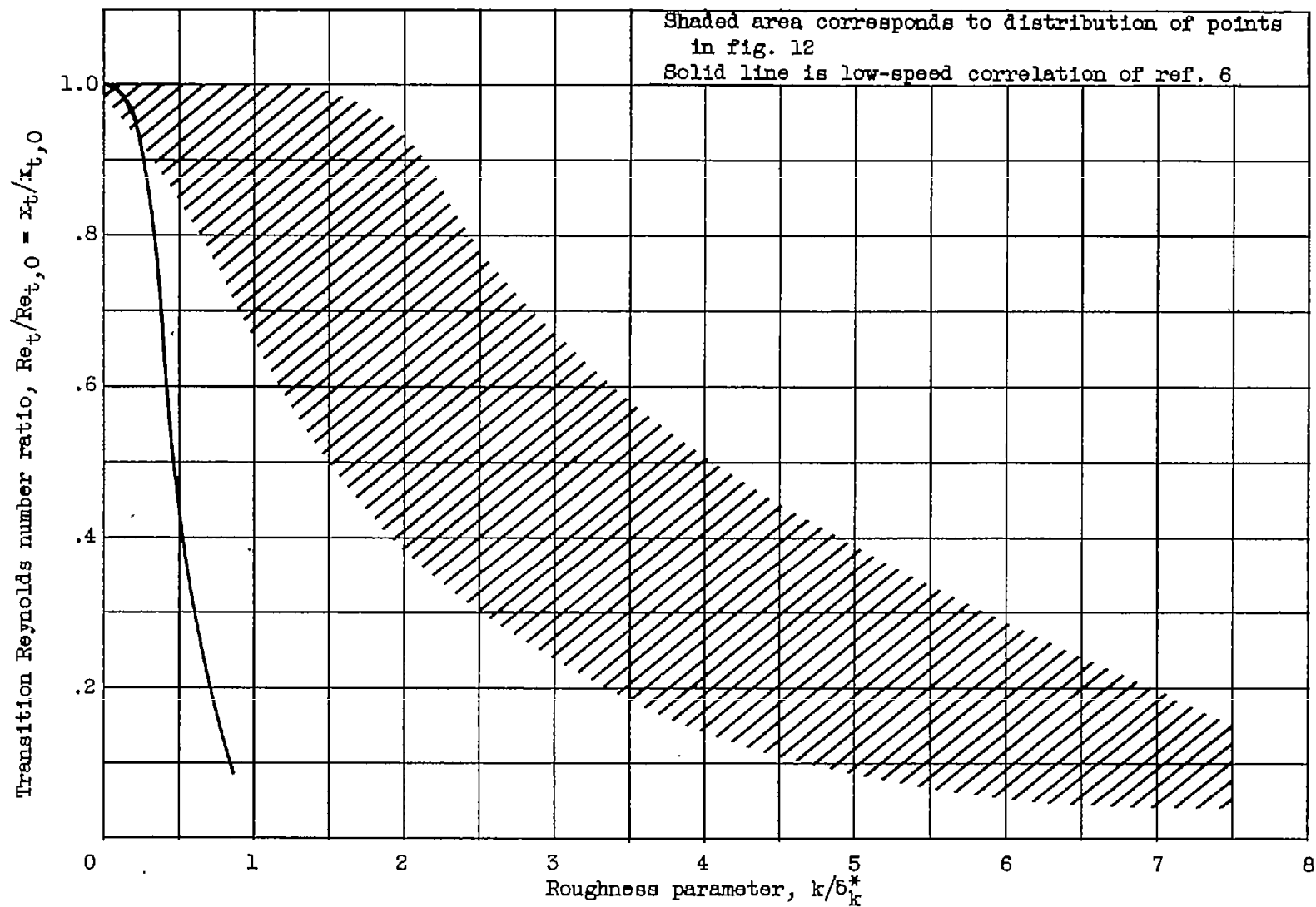
Figure 13. - Comparison of present roughness results with low-speed correlation of reference 6.